Atmospheric
Chemistry
and Physics

Role of a key microphysical factor in mixed-phase stratocumulus clouds and their interactions with aerosols

Seoung Soo Lee[1,2,3]**, Chang Hoon Jung**[4]**, Jinho Choi**[5]**, Young Jun Yoon**[6]**, Junshik Um**[5,7]**,
Youtong Zheng**[8]**, Jianping Guo**[9]**, Manguttathil G. Manoj**[10]**, and Sang-Keun Song**[11]

[1]Science and Technology Corporation, Hampton, Virginia, USA
[2]Earth System Science Interdisciplinary Center, University of Maryland, College Park, Maryland, USA
[3]Research Center for Climate Sciences, Pusan National University, Busan, Republic of Korea
[4]Department of Health Management, Kyungin Women's University, Incheon, Republic of Korea
[5]Department of Atmospheric Sciences, Pusan National University, Busan, Republic of Korea
[6]Division of Ocean and Atmosphere Sciences, Korea Polar Research Institute, Incheon, Republic of Korea
[7]Institute of Environmental Studies, Pusan National University, Busan, Republic of Korea
[8]Department of Earth and Atmospheric Sciences, University of Houston, Houston, Texas, USA
[9]State Key Laboratory of Severe Weather, Chinese Academy of Meteorological Sciences,
Beijing 100081, China
[10]Advanced Centre for Atmospheric Radar Research, Cochin University of Science and Technology,
Kerala, India
[11]Department of Earth and Marine Sciences, Jeju National University, Jeju, Republic of Korea

Correspondence: Seoung Soo Lee (cumulss@gmail.com, slee1247@umd.edu) and Sang-Keun Song
(songsk@jejunu.ac.kr)

Abstract. This study examines the ratio of ice crystal number concentration (ICNC) to cloud droplet number concentration (CDNC), that is ICNC / CDNC, in mixed-phase stratocumulus clouds. This examination is performed using a large-eddy simulation (LES) framework and is one of the efforts toward a more general understanding of mechanisms controlling cloud development and aerosol–cloud interactions, as well as the impacts of ice processes on them in mixed-phase stratocumulus clouds. For the examination, this study compares a case of polar mixed-phase stratocumulus clouds to one of midlatitude mixed-phase stratocumulus clouds with weak precipitation. It is found that ICNC / CDNC plays a critical role in causing differences in cloud development with respect to the relative proportion of liquid and ice mass between the cases by affecting in-cloud latent-heat processes. Note that this proportion has an important implication for cloud radiative properties and, thus, for climate. It is also found that ICNC / CDNC plays a critical role in causing differences in the interactions between clouds and aerosols and in the impacts of ice processes on clouds and their interactions with aerosols between the cases by affecting in-cloud latent-heat processes. Findings of this study suggest that ICNC / CDNC can be a simplified general factor that contributes to a more general understanding and parameterization of mixed-phase clouds, their interactions with aerosols and the roles of ice processes within them.

1 Introduction

Stratiform clouds (e.g., stratus and stratocumulus clouds) have significant impacts on climate (Warren et al., 1986; Stephens and Greenwald, 1991; Hartmann et al., 1992; Hahn and Warren, 2007; Wood, 2012; Dione et al., 2019; Zheng et al., 2021). Since industrialization, aerosol concentrations have increased, and this has had impacts on stratiform clouds and climate (Twomey, 1974; Albrecht, 1989; Ackerman et al., 2004). However, our level of understanding of these clouds and impacts has been low, and this has caused the highest uncertainty in the prediction of future climate (Ramaswamy et al., 2001; Forster et al., 2007; Knippertz et al., 2011; Hannak et al., 2017). Stratiform clouds can be classified into warm and mixed-phase clouds. Mixed-phase stratiform clouds involve ice processes and frequently form in midlatitude and polar regions. When mixed-phase clouds are associated with convective clouds, they can form even in tropical regions. Most previous studies have focused on warm clouds and their interactions with aerosols, whereas the mixed-phase stratiform clouds and their interactions with aerosols are poorly understood, mainly due to the more complex ice processes. Hence, mixed-phase stratiform clouds and their interactions with aerosols account for the uncertainty more than warm clouds and their interactions with aerosols (Ramaswamy et al., 2001; Forster et al., 2007; Wood, 2012; IPCC, 2021; Li et al., 2022).

The relative proportions of liquid mass, which can be represented by liquid-water content (LWC) or liquid-water path (LWP), and ice mass, which can be represented by ice-water content (IWC) or ice-water path (IWP), in mixed-phase stratiform clouds play a critical role in cloud radiative properties and, thus, in their climate feedbacks (Tsushima et al., 2006; Choi et al., 2010, 2014; Gettelman et al., 2012; Zhang et al., 2019). The relative proportion is defined to be IWC (IWP) over LWC (LWP) or IWC / LWC (IWP / LWP) in this study. Motivated by this and the above-mentioned uncertainty, this study aims to improve our understanding of mixed-phase stratiform clouds and their interactions with aerosols, with an emphasis on ice processes and IWC / LWC (or IWP / LWP).

Lee et al. (2021) have investigated mixed-phase stratocumulus clouds in a midlatitude region and found that microphysical latent-heat processes are more important in the development of mixed-phase stratiform clouds and their interactions with aerosols than entrainment and sedimentation processes. Lee et al. (2021) have found that a microphysical factor, the ratio of ice crystal number concentration (ICNC) to cloud droplet number concentration (CDNC) or ICNC / CDNC, plays an important role in latent processes, the development of mixed-phase stratiform clouds and their interactions with aerosols. In particular, Lee et al. (2021) have found that IWC / LWC or IWP / LWP is strongly affected by ICNC / CDNC. This is because water vapor deposits on the surface of ice crystals, while it condenses on droplets. As a result, ice crystals act as sources of depo-

sition, and droplets act as sources of condensation. Consequently, ice crystals act as sources of IWC (or IWP), and droplets act as sources of LWC (or LWP). More ice crystals and droplets provide the greater integrated surface area of ice crystals and droplets and induce more deposition and condensation, respectively, for a given environmental condition (Lee et al., 2009, 2021; Khain et al., 2012; Fan et al., 2018; Chua and Ming, 2020). A higher ICNC / CDNC means that there are more ice crystals or sources of deposition per droplet as sources of condensation in a given group of ice crystals and droplets. Thus, a higher ICNC / CDNC enables more deposition per unit of condensation to occur, which can raise IWC / LWC or IWP / LWP.

Mixed-phase stratocumulus clouds in different regions are known to have different IWC / LWC or IWP / LWP and aerosol–cloud interactions (e.g., Choi et al., 2010, 2014; Zhang et al., 2019). Lots of factors, such as environmental conditions, which can be represented by variables such as temperature, humidity and wind shear, and macrophysical factors, one of which is the relative location of ice crystal and droplet layers, can explain those differences. Choi et al. (2010, 2014) and Zhang et al. (2019) have shown that, as temperature lowers, IWC / LWC or IWP / LWP tends to increase, and they indicated that temperature is a primary environmental condition that can be used to explain the differences in IWC / LWC among different regions or clouds. However, Choi et al. (2010, 2014) and Zhang et al. (2019) have not discussed process-level mechanisms that govern the role of temperature in those differences.

It is important to establish a general principle that explains the differences in LWC / LWC and in aerosol–cloud interactions among regions since the general principle is useful in the development of a more general or comprehensive parameterization of stratocumulus clouds and their interactions with aerosols for climate models. This contributes to the better prediction of future climate considering the fact that the absence of the comprehensive parameterization has been considered to be one of the biggest obstacles with regard to better prediction (Ramaswamy et al., 2001; Foster et al., 2007; Stevens and Feingold, 2009).

As a way of contributing to the establishment of the general principle, this study attempts to take ICNC / CDNC as a general factor, which can constitute the general principle, to explain the differences in IWC / LWC (or IWP / LWP) and in aerosol–cloud interactions among clouds. This study also attempts to elucidate how ice processes differentiate mixed-phase stratiform clouds from warm clouds in terms of cloud development and its interactions with aerosols and how this differentiation varies among cases of mixed-phase stratiform clouds with different ICNC / CDNC values. This attempt is valuable considering that, in general, the establishment of the general principle for stratocumulus clouds and their interactions with aerosols has progressed much less than that for other types of clouds, such as convective clouds, and their interactions with aerosols. Furthermore, the attempt is also

seen to be valuable when considering the fact that our level of understanding of how ice processes differentiate mixed-phase stratiform clouds and their interactions with aerosols from much-studied warm clouds and their interactions with aerosols has been low. Here, we want to emphasize that this study does not aim to gain a fully established general principle but rather aims to test the factor that can be useful in moving ahead on our path to a more complete general principle. Hence, this study should be regarded to be a steppingstone towards the established principle and should not be considered to be a perfect study that gets us the fully established principle. Taking into account the fact that even attempts to provide general factors for the general principle have been rare, the fulfillment of the aim is likely to provide us with valuable preliminary information that streamlines the development of a more established general principle.

For the attempt, this study investigates a case of mixed-phase stratiform clouds in the polar region. Via the investigation, this study aims to identify process-level mechanisms that control the development of those clouds and their interactions with aerosols and the impact of ice processes on this development and these interactions using a large-eddy simulation (LES) framework. Then, this study compares the mechanisms in the case of polar clouds to those in a case of midlatitude clouds which have been examined by Lee et al. (2021). This comparison is based on Choi et al. (2010, 2014) and Zhang et al. (2019), who have shown that temperature is an important factor which explains the differences in IWC / LWC among regions or clouds. Due to significant differences in latitudes, noticeable differences in the temperature of air are seen between the polar and midlatitude cases. Hence, through this comparison, this study looks at the role of temperature in those differences in IWC / LWC and associated aerosol–cloud interactions. More importantly than that, as a way of identifying process-level mechanisms that control the role of temperature, this study tests how ICNC / CDNC as the general factor is linked to the role of temperature using the LES framework. Through this test, this study also identifies process-level mechanisms that control how ICNC / CDNC affects the roles of ice processes in the differentiation between mixed-phase stratiform and warm clouds in terms of cloud development and its interactions with aerosols and how it causes the variation in the differentiation between the cases of mixed-phase stratiform clouds.

2   Case, model and simulations

2.1   LES model

LES simulations are performed by using the Advanced Research Weather Research and Forecasting (ARW) model. A bin scheme, which is detailed in Khain et al. (2000, 2011), is adopted by the ARW for the simulation of microphysics. Size distribution functions for each class of hydrometeors, which are classified into water drops, ice crystals (plate, colum-

nar and branch types), snow aggregates, graupel and hail, are represented with 33 mass-doubling bins; i.e., the mass of a particle m_k in the kth bin is determined as $m_k = 2m_{k-1}$. Each of the hydrometeors has its own terminal velocity that varies with the hydrometeor mass, and the sedimentation of hydrometeors is simulated using their terminal velocity.

Size distribution functions for aerosols, which act as cloud condensation nuclei (CCN) and ice-nucleating particles (INPs), adopt the same mass-doubling bins as for hydrometeors. The evolution of aerosol size distribution and the associated aerosol concentrations at each grid point are controlled by aerosol sinks and sources such as aerosol advection, turbulent mixing, activation, and aerosol regeneration via the evaporation of droplets and the sublimation of ice crystals. Aerosol regeneration follows a method that is similar to that described in Xue et al. (2010). It is assumed that aerosols do not fall down by themselves and move around by airflow that is composed of horizontal flow, updrafts, downdrafts and turbulent motions. When aerosols move with airflow, it is assumed that they move with the same velocity as airflow. Taking activation as an example of the evolution of aerosol size distribution, the bins of the aerosol spectra that correspond to activated particles are emptied. Activated aerosol particles are included in hydrometeors and move to different classes and sizes of hydrometeors through collision–coalescence. In case hydrometeors with aerosol particles precipitate to the surface, those particles are removed from the atmosphere.

The large energetic turbulent eddies are directly resolved by the LES framework, and the effects of the smaller subgrid-scale turbulent motions on the resolved flow are parameterized based on the most widely used method that Smagorinsky (1963) and Lilly (1967) proposed. In this method, the mixing timescale is defined to be the norm of the strain rate tensor (Bartosiewicz and Duponcheel, 2018). A cloud droplet nucleation parameterization based on Köhler theory represents cloud droplet nucleation. Arbitrary aerosol mixing states and aerosol size distributions can be fed into this parameterization. To represent heterogeneous ice crystal nucleation, the parameterizations by Lohmann and Diehl (2006) and Möhler et al. (2006) are used. In these parameterizations, contact, immersion, condensation–freezing and deposition nucleation paths are all considered by taking into account the size distribution of INPs, temperature and supersaturation. Homogeneous aerosol (or haze particle) and droplet freezing is also considered following the theory developed by Koop et al. (2000).

The bin microphysics scheme is coupled to the Rapid Radiation Transfer Model (RRTM; Mlawer et al., 1997). The effective sizes of hydrometeors, which are calculated in the bin scheme, are fed into the RRTM as a way of considering the effects of the effective sizes on radiation. The surface process and resultant surface heat fluxes are simulated by the interactive Noah land surface model (Chen and Dudhia, 2001).
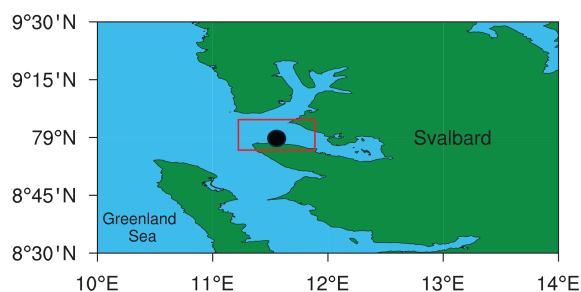
Figure 1. A red rectangle marks the simulation domain in the Svalbard area in Norway, and a dot in the rectangle marks a ground station which is a part of the Cloudnet observation network. The light blue represents the ocean, and the green represents the land area.

2.2 Case and simulations

2.2.1 Case and standard simulations

In the Svalbard area in Norway, a system of mixed-phase stratocumulus clouds existed over the horizontal domain marked by a red rectangle in Fig. 1 and during a period between 02:00 and 10:00 local solar time (LST) on 29 March 2017. These clouds are observed by a ground station which is a part of the Cloudnet observation network, marked by a dot in Fig. 1. The Cloudnet observation network was established to provide a systematic evaluation of clouds in forecast and climate models. The Cloudnet observation network aims to establish a number of ground-based remote sensing sites, which would all be equipped with a specific array of instrumentation, using sensors such as radiometer, lidar and Dopplerized millimeter wave radar in order to provide vertical profiles of the main cloud variables (e.g., LWC and IWC) (Hogan et al., 2007). In the Cloudnet observation network, in particular, LWC is measured by a radiometer with a spatial resolution of ~ 50 m in the vertical direction and a temporal resolution of 30 s. The retrieval of IWC is performed by using radar reflectivity and lidar backscatter in the Cloudnet observation network with a spatial resolution of ~ 10 m in the vertical direction and a temporal resolution of 30 s, as described in Donovan et al. (2001), Donovan and Lammeren (2001), Donovan (2003), and Tinel et al. (2005). In the retrieval, the lidar signal and radar reflectivity profiles are combined and inverted using a combined lidar–radar equation as a function of the light extinction coefficient and radar reflectivity. The combined equation is detailed in Donovan and Lammeren (2001). In the Cloudnet data, LWC data, with a coarser spatial resolution than IWC data, are interpolated to observation locations of IWC data, and IWP and LWP data are obtained from these IWC and interpolated LWC data, respectively. The Cloudnet observation data, including these IWC, LWC, IWP and LWP data, are provided to the public at a temporal resolution of 30 s in a continuous manner. This study utilizes these publicized Cloudnet data.

On average, the bottom and top of the observed clouds, which are measured by radar and lidar in the Cloudnet observation network, are at ~ 400 m and ~ 3 km in altitude, respectively. The simulation of the observed system or case, i.e., the control run, is performed three-dimensionally over the red rectangle and during the period between 02:00 and 10:00 LST on 29 March 2017. The horizontal domain adopts a 100 m resolution for the control run. The length of the domain in the horizontal directions is 50 km. The length of the domain in the vertical direction is ~ 5 km, and the resolution for the vertical domain gets coarsened with height from ~ 5 m just above the surface to ~ 150 m at the model top, as detailed in the Supplement. Reanalysis data, which are produced by the Met Office Unified Model (Brown et al., 2012) every 6 h on a $0.11° \times 0.11°$ grid, provide potential temperature, specific humidity and wind as initial and boundary conditions, which represent the synoptic-scale environment, for the control run. The control run employs an open lateral boundary condition. Figure 2a shows the vertical distribution of the domain-averaged potential temperature and humidity in those reanalysis data at the first time step. A neutral, mixed layer is between the surface and 1 km in altitude as an initial condition (Fig. 2a). Figure 2b shows the time evolution of the domain-averaged large-scale subsidence or downdraft in the reanalysis data and at the model top. This large-scale subsidence is imposed on the control run as a part of background wind fields and interacts with updrafts and downdrafts generated by relatively small-scale processes, including those associated with clouds. The large-scale subsidence is gradually reduced with time (Fig. 2b). Figure 2c shows the time evolution of the domain-averaged surface temperature in the reanalysis data. This evolution of the surface temperature is strongly controlled by the sea surface temperature considering the fact that a large portion of the red-rectangle domain is accounted for by the ocean (Fig. 1). Due to the sunrise, the surface temperature starts to increase more rapidly around 08:00 LST (Fig. 2c).

The properties of cloud condensation nuclei (CCN), such as the number concentration, size distribution and composition, are measured in the domain (Tunved et al., 2013; Jung et al., 2018). The measurement of the CCN concentration was carried out at the location marked by a dot in Fig. 1 using the commercial Droplet Measurement Technologies CCN counter with one column (CCNC-100), managed by the Korea Polar Research Institute since 2007. The CCNC-100 measures the CCN concentration at supersaturations of 0.2 %, 0.4 %, 0.6 %, 0.8 % and 1 % (Jung et al., 2018). The aerosol number size distribution is observed using a closed-loop differential mobility particle sizer (DMPS). The DMPS charges aerosol particles and exposes them to an electric field, which causes them to experience a force proportional to their electrical mobility, resulting in their classification according to size (Tunved et al., 2013). Aerosol composition is measured using aerosol mass spectrometry (AMS). The
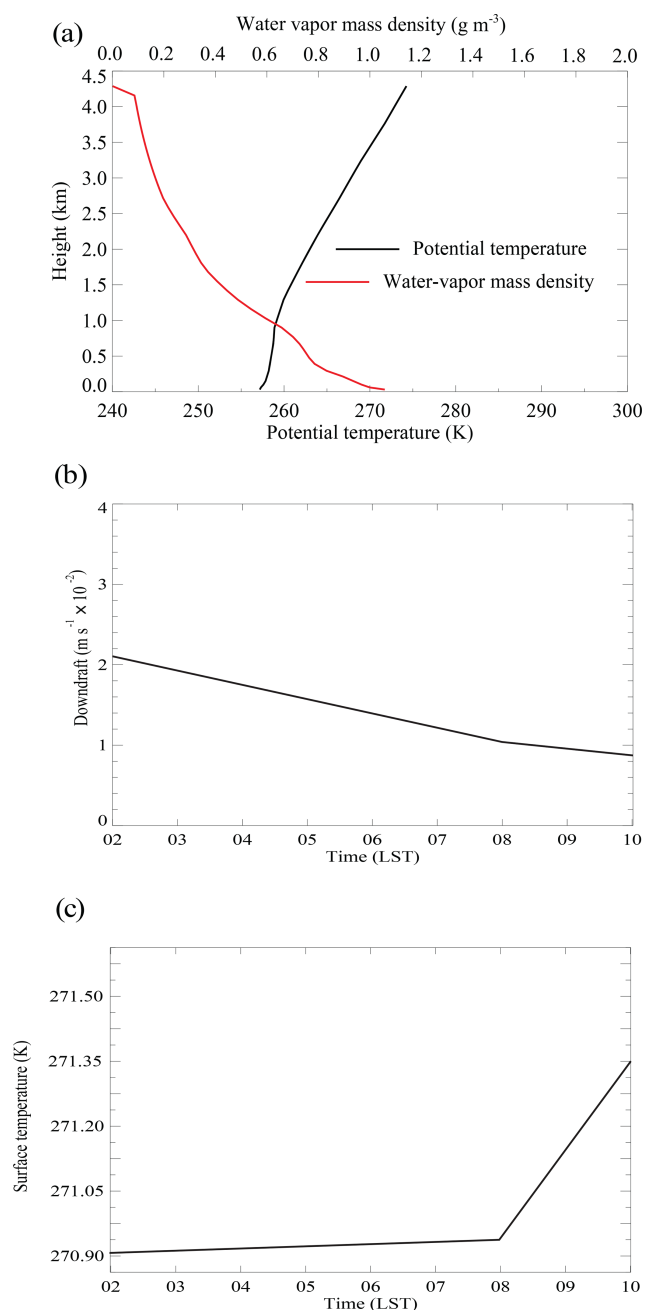
Figure 2. (a) The vertical distributions of the domain-averaged potential temperature and humidity at the first time step, **(b)** the time series of the domain-averaged large-scale subsidence or downdraft at the model top, and **(c)** the time series of the domain-averaged surface temperature.

AMS measures the composition by vaporizing and ionizing aerosol particles.

The measurement indicates that, on average, aerosol particles are an internal mixture of 70 % ammonium sulfate and 30 % organic compound. This mixture is assumed to represent aerosol chemical composition over the whole domain

and simulation period for this study. The observed and averaged concentration of aerosols acting as CCN is $\sim 200 \, \text{cm}^{-3}$ over the simulation period between 02:00 and 10:00 LST on 29 March 2017. Note that the average of a variable with respect to time in the rest of this paper is calculated over this period between 02:00 and 10:00 LST, unless otherwise stated. As the averaged concentration of aerosols acting as CCN, $200 \, \text{cm}^{-3}$ is interpolated into all of grid points immediately above the surface at the first time step.

This study does not take into account aerosol effects on radiation before aerosols are activated since no significant number of radiation absorbers is found in the mixture. Based on observations, the size distribution of aerosols acting as CCN is assumed to be a tri-modal log-normal distribution (Fig. 3). The shape of the distribution, which is a tri-modal log-normal distribution, as shown in Fig. 3, is applied to the size distribution of aerosols acting as CCN in all parts of the domain during the whole simulation period. The assumed shape in Fig. 3 is obtained by calculating the average based on the observed size distribution parameters (i.e., modal radius and standard deviation of each of the nuclei, accumulation and coarse modes, and the partitioning of aerosol number among those modes) over the simulation period. Note that, although these parameters and/or the shape of the aerosol size distribution do not vary, associated aerosol concentrations vary over the simulation domain and period via the processes described in Sect. 2.1. This study makes an assumption that the interpolated CCN concentrations do not vary with height in a layer between the surface and the planetary boundary layer (PBL) top around 1 km in altitude at the first time step, following previous studies such as Gras (1991), Jaenicke (1993), and Seinfeld and Pandis (1998). However, above the PBL top, they are assumed to decrease exponentially with height at the first time step based on those previous studies, although the shapes of the size distribution and composition do not change with height. It is assumed that the properties of INPs and CCN are not different, except for the concentrations. The concentration of aerosols acting as CCN is assumed to be 100 times higher than that of aerosols acting as INPs over grid points at the first time step based on a general difference in concentrations between CCN and INPs (Pruppacher and Klett, 1978). Hence, the concentration of aerosols acting as INPs at the first time step is $2 \, \text{cm}^{-3}$ in the control run. This assumed concentration of aerosols acting as INPs is higher than usual (Seinfeld and Pandis, 1998). However, Hartmann et al. (2021) observed an INP concentration that was of the same order of magnitude as that assumed here in the Svalbard area when strong dust events occurred, meaning that the assumed INP concentration is not that unrealistic.

To examine the effects of aerosols on mixed-phase clouds, the control run is repeated by increasing the concentration of aerosols by a factor of 10. In the repeated (control) run, the initial concentrations of aerosols acting as CCN and INPs at grid points immediately above the surface are 2000 (200)
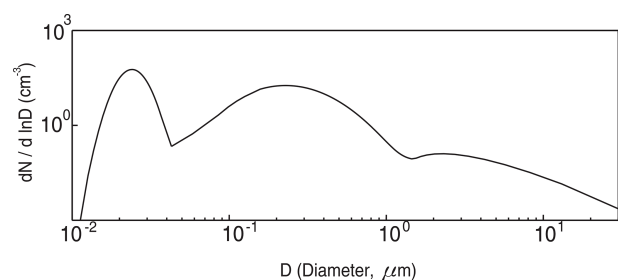
Figure 3. Aerosol size distribution at the surface. N represents aerosol number concentration per unit volume of air, and D represents aerosol diameter.

Figure 4. The vertical distributions of the time- and domain-averaged IWC and LWC in the 200_2 and 200_0 runs.

and 20 (2) cm^{-3}, respectively. Reflecting these concentrations in the simulation name, the control run is referred to as the "200_2 run", and the repeated run is referred to as the "2000_20 run". To isolate the effects of aerosols acting as CCN (INPs) on mixed-phase clouds, the control run is repeated again by increasing the concentration of aerosols acting as CCN (INPs) only (and not INPs (CCN)) by a factor of 10. In this repeated run, with the increase in the concentration of aerosols acting as CCN (INPs), the initial concentrations of aerosols acting as CCN and INPs at grid points immediately above the surface are 2000 (200) and 2 (20) cm^{-3}, respectively. Reflecting this, the repeated run is referred to as the "2000_2 (200_20) run".

2.2.2 Additional simulations

To isolate the impacts of ice processes on the adopted case and its interactions with aerosols, the 200_2 and 2000_2 runs are repeated by removing ice processes. These repeated runs are referred to as the 200_0 and 2000_0 runs. In the 200_0 and 2000_0 runs, all hydrometeors (i.e., ice crystals, snow, graupel and hail), phase transitions (e.g., deposition and sublimation) and aerosols (i.e., INPs) which are associated with ice processes are removed. Hence, in these runs, only droplets (i.e., cloud liquid), raindrops, associated phase transitions (e.g., condensation and evaporation) and aerosols acting as CCN are present, regardless of temperature. Stated differently, these noice runs simulate the warm-cloud counterpart of the selected mixed-phase cloud system. Via comparisons between a pair of the 200_2 and 2000_2 runs and a pair of the 200_0 and 2000_0 runs, the role of ice processes in the differentiation between mixed-phase and warm clouds is to be identified. Along with this identification, the role of the interplay between ice crystals and droplets in the development of the selected mixed-phase cloud system and its interactions with aerosols is to be isolated.

As detailed in Sect. 3.1.4 and 3.2.2 below, the test of ICNC / CDNC as a general factor requires more simulations to see the impacts of ICNCavg / CDNCavg on clouds and their interactions with aerosols. Here, ICNCavg and CD-NC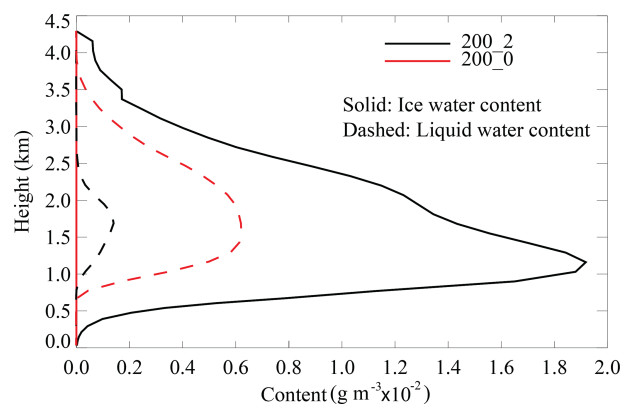avg represent the average ICNC and CDNC over grid points and time steps with non-zero ICNC and CDNC, respectively. ICNCavg / CDNCavg represents the overall ICNC / CDNC over the domain and simulation period. To respond to this requirement, the 200_0.07, 2000_0.07 and 200_0.7 runs are performed, and their details are given in Sect. 3.1.4 and 3.2.2. In addition, all the simulations above are repeated by turning off radiative processes, and Sect. 3.3 provides the details of these repeated simulations. These repeated runs are the 200_2_norad, 2000_20_norad, 2000_2_norad, 200_20_norad, 200_0_norad, 2000_0_norad, 200_0.07_norad, 2000_0.07_norad and 200_0.7_norad runs. Moreover, based on the argument in Sect. 4.2, the 4000_45, 13_0.1, 4000_1.8 and 12_0.0035 runs are performed, and details of these runs are provided in Sect. 4.2. Some of the simulations are summarized in Table 1 for better clarification, with a brief description of their configuration.

3 Results

3.1 The 200_2 run vs. the 200_0 run

3.1.1 Model validation

This study adopts the Cloudnet observation, which has been used to assess cloud simulations, as in Illingworth et al. (2007) and Hansen et al. (2018), to evaluate the 200_2 run. Simulated LWP and IWP, as shown in Fig. 4 and Table 2, are compared to the observed LWP and retrieved IWP in the Cloudnet data, respectively. The average LWP over all time steps and grid columns for the period between 02:00 and 10:00 LST on 29 March 2017 is 1.23 g m^{-2} in the 200_2 run and 1.12 g m^{-2} in the Cloudnet observation. The average IWP over all time steps and grid columns over the period is 31.94 g m^{-2} in the 200_2 run and 29.10 g m^{-2} in the retrieval. Cloud bottom height, which is averaged over grid columns and time steps with non-zero cloud bottom height over the period, is 420 m in the 200_2 run and 440 m in the Cloudnet observation. Cloud top height, which is averaged

Table 1. Summary of simulations.

Simulations	The number concentration of aerosols acting as CCN at the first time step in the PBL (cm^{-3})	The number concentration of aerosols acting as INPs at the first time step in the PBL (cm^{-3})	ICNCavg / CDNCavg	Ice processes	Radiation
200_2	200	2	0.220	Present	Present
2000_20	2000	20	0.201	Present	Present
2000_2	2000	2	0.108	Present	Present
200_20	200	20	0.512	Present	Present
200_0	200	2	0.000	Absent	Present
2000_0	2000	2	0.000	Absent	Present
200_0.07	200	0.07	0.022	Present	Present
2000_0.07	2000	0.07	0.012	Present	Present
200_0.7	200	0.7	0.041	Present	Present
4000_45	4000	45	0.220	Present	Present
13_0.1	13	0.1	0.220	Present	Present
4000_1.8	4000	1.8	0.022	Present	Present
12_0.0035	12	0.0035	0.022	Present	Present

Table 2. The averaged IWC, LWC, IWP, LWP, condensation and deposition rates over all of the grid points and during the simulation period in each of simulations. IWC / LWC (IWP / LWP) is the averaged IWC (IWP) over the averaged LWC (LWP). Also, shown are the vertically integrated condensation and deposition rates over each cloudy column, which are averaged over those columns and the simulation period. The average cloud base sedimentation rate, which is for each of the ice crystals and droplets, over the cloud base and simulation period and the average cloud top entrainment rate over the cloud top and simulation period are shown as well.

Simulations	IWC (10^{-3} g m^{-3})	LWC (10^{-3} g m^{-3})	IWP (g m^{-2})	LWP (g m^{-2})	IWC / LWC	IWP / LWP	Condensation rate Over grid points (10^{-2} g m^{-3} s^{-1})	Condensation rate Over cloudy columns (g m^{-2} s^{-1})	Deposition rate Over grid points (10^{-2} g m^{-3} s^{-1})	Deposition rate Over cloudy columns (g m^{-2} s^{-1})	Cloud base sedimentation (10^{-3} g m^{-2} s^{-1}) Ice crystal	Cloud base sedimentation Droplet	Entrainment (cm s^{-1})
200_2	6.57	0.25	31.94	1.23	26.28	25.96	0.11	1.98	1.30	23.40	1.17	0.17	0.25
2000_20	7.82	0.21	40.91	1.08	37.24	37.91	0.09	1.62	1.57	28.26	0.94	0.06	0.53
2000_2	6.55	0.29	31.85	1.46	22.58	21.81	0.12	2.16	1.28	23.04	1.11	0.08	0.28
200_20	7.80	0.20	40.82	1.01	39.00	40.42	0.09	1.62	1.56	28.08	0.97	0.11	0.51
200_0	0.00	2.06	0.00	10.35	0.00	0.00	0.72	12.48	0.00	0.00	0.00	0.36	0.08
2000_0	0.00	2.25	0.00	11.29	0.00	0.00	0.76	12.80	0.00	0.00	0.00	0.14	0.10
200_0.07	0.89	0.85	4.27	4.20	1.05	1.02	0.32	5.76	0.35	6.30	0.19	0.28	0.06
2000_0.07	0.79	0.97	3.82	4.83	0.81	0.79	0.38	6.84	0.31	5.58	0.17	0.19	0.07
200_0.7	0.98	0.78	4.73	3.88	1.25	1.22	0.31	5.58	0.39	7.02	0.14	0.22	0.07

over grid columns and time steps with non-zero cloud top height over the period, is 3.5 km in the 200_2 run and 3.3 km in the Cloudnet observation. The LWP and cloud bottom and cloud top heights each show a $\sim 10\%$ difference between the 200_2 run and the observations. IWP also shows a $\sim 10\%$ difference between the 200_2 run and the retrieval. Thus, the 200_2 run is considered to have performed reasonably well for these variables.

To provide additional information regarding cloud development, Fig. 5 shows the time evolution of the simulated and observed cloud top and cloud bottom heights, simulated and retrieved IWP, and simulated and observed LWP, together with the evolution of the simulated surface sensible- and latent-heat fluxes; the simulated evolutions in Fig. 5 are from the 200_2 run. This is based on the fact that the cloud top and cloud bottom heights, IWP, and LWP are considered

to be good indicators of cloud development, and the surface fluxes are considered to be important parameters controlling the overall development of clouds. The cloud top height increases between 02:00 and ∼ 05:00 LST, and, after ∼ 05:00 LST, it decreases gradually. The cloud bottom height decreases between 02:00 and ∼ 05:00 LST, and, after ∼ 05:00 LST, it does not change much. IWP and LWP show an overall increase between 02:00 and ∼ 05:30 LST, reaching their peak around 05:30 LST and then showing an overall decrease. The surface fluxes decrease with time, although the reduction rate of the fluxes starts to decrease around 08:00 LST in association with the rapid increase in the surface temperature which starts around 08:00 LST, as shown in Fig. 2c.

The time- and domain-averaged IWP is ∼ 1 order of magnitude greater than LWP, and the time- and domain-averaged IWC is ∼ 1 order of magnitude greater than LWC in the 200_2 run (Fig. 4 and Table 2). For the sake of simplicity, henceforth, the averaged IWC over the averaged LWC is denoted by IWC / LWC, and the averaged IWP over the averaged LWP is denoted by IWP / LWP. In the 200_2 run, IWC / LWC is 26.28, and IWP / LWP is 25.96. Since IWP and LWP are vertically integrated IWC and LWC over the vertical domain, respectively, the qualitative nature of differences between IWC and LWC is not very different from that of differences between IWP and LWP. Hence, mentioning both a pair of IWC and LWC and a pair of IWP and LWP is considered to be redundant, and mentioning either a pair of IWC and LWC or a pair of IWP and LWP enhances the readability. Henceforth, IWC and LWC are chosen to be mentioned in the text, although the entireties of IWC, LWC, IWP and LWP are displayed in Tables 2 and 3.

Choi et al. (2014) and Zhang et al. (2019) have obtained the supercooled cloud fraction (SCF), which is basically the ratio of LWC to the sum of LWC and IWC and is denoted by LWC / (LWC+IWC) using satellite- and ground-observed data collected over the period of ∼ 1 year to ∼ 5 years. Choi et al. (2014) have shown that SCF is as low as ∼ 0.01 for the temperature range between −16 and −33 °C. Zhang et al. (2019) have also shown that SCF is as low as ∼ 0.03 for the same temperature range, although the occurrence of SCF of ∼ 0.03 or lower is rare. Note that the average air temperature immediately below the cloud base and above the cloud top over the simulation period is −16 and −33 °C, respectively, in the 200_2 run, and SCF in the 200_2 run is 0.04. Hence, based on Choi et al. (2014) and Zhang et al. (2019), we believe that SCF in the 200_2 run is observable and thus not that unrealistic, although it may not occur frequently.

3.1.2 Microphysical processes, sedimentation and entrainment

To understand process-level mechanisms that control the results, microphysical processes are analyzed. As indicated by Ovchinnikov et al. (2011), in clouds with weak precipitation,
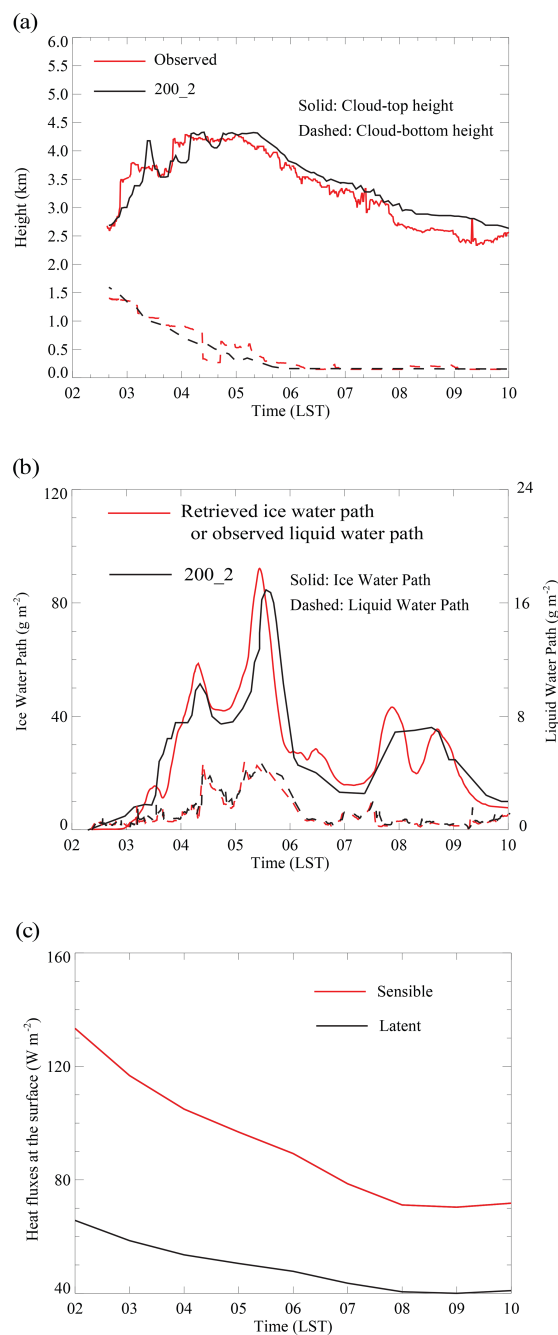

Figure 5. The time series of **(a)** observed and simulated cloud top and cloud bottom heights, **(b)** retrieved and simulated IWP and observed and simulated LWP, and **(c)** the simulated surface sensible- and latent-heat fluxes. Observed and retrieved values are from the ground station, as marked in Fig. 1. For the time series, in the simulation domain, the simulated cloud top height is averaged over grid points with cloud tops, and the simulated cloud bottom height is averaged over grid points with cloud bottoms, while the simulated IWP and LWP are averaged over grid points with non-zero IWP and LWP, respectively, at each time step in the 200_2 run. The simulated surface sensible- and latent-heat fluxes are averaged over the horizontal domain at the surface and over each time step in the 200_2 run.

Table 3. Same as Table 2 but for the repeated simulations with radiative processes turned off.

Simulations	IWC (10^{-3} g m^{-3})	LWC (10^{-3} g m^{-3})	IWP (g m^{-2})	LWP (g m^{-2})	IWC / LWC	IWP / LWP	Condensation rate		Deposition rate		Cloud base sedimentation (10^{-3} g m^{-2} s^{-1})		Entrainment (cm s^{-1})
							Over grid points (10^{-2} g m^{-3} s^{-1})	Over cloudy columns (g m^{-2} s^{-1})	Over grid points (10^{-2} g m^{-3} s^{-1})	Over cloudy columns (g m^{-2} s^{-1})	Ice crystal	Droplet	
200_2_norad	6.42	0.24	31.21	1.22	26.75	25.58	0.10	1.96	1.29	23.35	1.16	0.16	0.24
2000_20_norad	7.63	0.21	40.05	1.07	36.33	37.42	0.09	1.59	1.55	29.91	0.92	0.06	0.51
2000_2_norad	6.40	0.29	31.11	1.45	22.06	21.45	0.11	2.12	1.26	22.69	1.07	0.08	0.27
200_20_norad	7.61	0.20	39.95	0.99	38.05	40.35	0.09	1.59	1.54	27.72	0.97	0.11	0.49
200_0_norad	0.00	2.03	0.00	10.20	0.00	0.00	0.72	12.31	0.00	0.00	0.00	0.34	0.08
2000_0_norad	0.00	2.21	0.00	11.12	0.00	0.00	0.75	12.63	0.00	0.00	0.00	0.13	0.10
200_0.07_norad	0.87	0.84	4.21	4.17	1.04	1.01	0.31	5.74	0.35	6.21	0.18	0.27	0.05
2000_0.07_norad	0.78	0.96	3.78	4.80	0.81	0.79	0.36	6.81	0.30	5.50	0.16	0.18	0.06
200_0.7_norad	0.97	0.76	4.70	3.85	1.25	1.22	0.30	5.55	0.38	6.91	0.13	0.21	0.06

a high degree of correlation is found between IWC and deposition or between LWC and condensation considering the fact that deposition is the source of IWC and condensation is the source of LWC. In the 200_2 run, the average surface precipitation rate over the simulation period is ~ 0.0020 mm h^{-1}, which can be considered to be weak. Hence, in this case, condensation is considered to be a proxy for LWC, and deposition is considered to be a proxy for IWC. Based on this, to gain a process-level understanding of microphysical processes that control the simulated LWC and IWC, condensation and deposition are analyzed.

As seen in Fig. 6 and Table 2, the average deposition rate is ~ 1 order of magnitude greater than the condensation rate in the 200_2 run, leading to much greater IWC than LWC in the 200_2 run. This is in contrast to the situation in the case of mixed-phase stratocumulus clouds, which were located in a midlatitude region, in Lee et al. (2021). In that case, henceforth, the average IWC and LWC are of the same order of magnitude. For the sake of brevity, the case in Lee et al. (2021) is referred to as the "midlatitude case", while the case of mixed-phase clouds, which is adopted by this study, in the Svalbard area is referred to as the "polar case". In the midlatitude case, IWC / LWC is 1.55, which is ~ 1 order of magnitude smaller than that in the polar case.

Warm clouds in the 200_0 run show that the time- and domain-averaged condensation rates are lower than the time- and the domain-averaged sum of the condensation and deposition rates in the 200_2 run (Fig. 6 and Table 2). This leads to a situation where warm clouds in the 200_0 run show the time- and domain-averaged LWC that is lower than the time- and domain-averaged water content (WC), which is the sum of IWC and LWC, in mixed-phase clouds in the 200_2 run (Fig. 4 and Table 2). This is despite the fact that LWC in the 200_0 run is higher than LWC in the 200_2 run (Fig. 4 and Table 2); WC represents the total cloud mass in mixed-phase
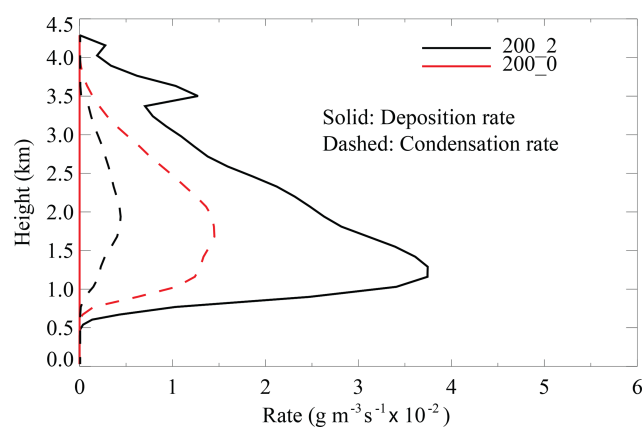
Figure 6. The vertical distributions of the time- and domain-averaged deposition and condensation rates in the 200_2 and 200_0 runs.

clouds, while LWC alone represents the total cloud mass in warm clouds.

It should be noted that the average rate of sedimentation of droplets over the cloud base and simulation period decreases from the 200_0 run to the 200_2 run (Table 2). This is mainly due to the decrease in LWC from the 200_0 run to the 200_2 run. The average rate of sedimentation of ice crystals over the cloud base and simulation period increases from the 200_0 run to the 200_2 run since the sedimentation of ice crystals is absent in the 200_0 run (Table 2). The average entrainment rate over the cloud top and simulation period increases from the 200_0 run to the 200_2 run (Table 2). Here, entrainment rate is defined to be the difference between the rate of increase in cloud top height and the large-scale subsidence, following Moeng et al. (1999), Jiang et al. (2002), Stevens et al. (2003a, b) and Ackerman et al. (2004). Entrainment tends to reduce the total cloud mass more in the

200_2 run than in the 200_0 run. Thus, entrainment should be opted out when it comes to mechanisms leading to the increase in the total cloud mass from the 200_0 run to the 200_2 run. Here, the vertical integration of each of the condensation and deposition rates is obtained over each cloudy column in the domain for each of the runs. For the sake of brevity, these vertical integrations of condensation and deposition rates are referred to as the integrated condensation and deposition rates, respectively. Then, each of the integrated condensation and deposition rates are averaged over cloudy columns and the simulation period. It is found that the average rate of the droplet sedimentation over the cloud base and simulation period is ∼ 4 orders of magnitude smaller than the average integrated condensation rate in the 200_2 run (Table 2). The average rate of the ice crystal sedimentation over the cloud base and simulation period is ∼ 4 orders of magnitude smaller than the average integrated deposition rate in the 200_2 run (Table 2). It is also found that the average rate of the droplet sedimentation over the cloud base and simulation period is ∼ 5 orders of magnitude smaller than the average integrated condensation rate in the 200_0 run (Table 2). Changes in the average rate of the droplet sedimentation over the cloud base and simulation period are ∼ 4 to 5 orders of magnitude smaller than those in the average integrated condensation rate between the 200_2 and 200_0 runs (Table 2). Changes in the average rate of the ice crystal sedimentation over the cloud base and simulation period are ∼ 4 to 5 orders of magnitude smaller than those in the average integrated deposition rate between the 200_2 and 200_0 runs (Table 2). Thus, condensation and deposition, but not the droplet and ice crystal sedimentation, are the main factors controlling cloud mass, which is represented by LWC and IWC, and the total cloud mass in the 200_2 and 200_0 runs. The variations in cloud mass and the total cloud mass between the runs are also mainly controlled by condensation and deposition but not by droplet and ice crystal sedimentation. These dominant roles of condensation and deposition over those of droplet and ice crystal sedimentation are observed in the midlatitude case and its warm-cloud counterpart as well.

3.1.3 Hypothesis

We hypothesized that ICNC / CDNC can be an important factor that determines the above-described differences between the polar and midlatitude cases. Note that in both the polar and the midlatitude cases, pockets of ice particles and those of liquid particles are mixed together instead of being separated from each other, as seen in Fig. 4 and Lee et al. (2021). Remember that ice crystals are more sources of deposition per droplet when ICNC / CDNC is higher. Thus, as ICNC / CDNC increases in a situation where qv > qsw (here, qv and qsw represent water vapor pressure and water vapor saturation pressure for liquid water or droplets, respectively), it is likely that the portion of water vapor, which is
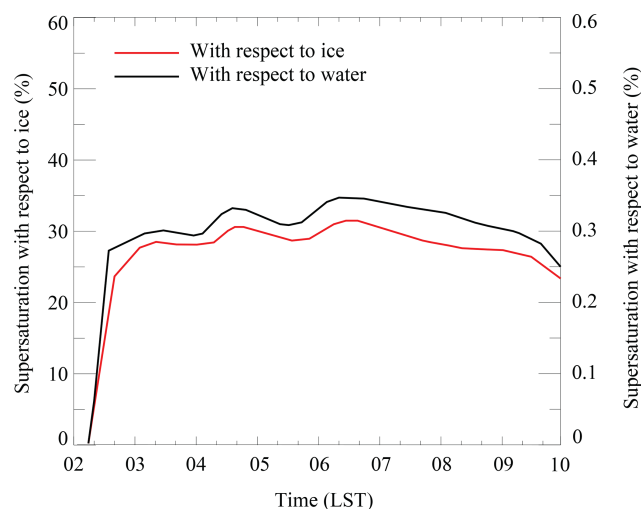

Figure 7. The time series of the average supersaturation with respect to ice and water over grid points where deposition occurs in the presence of both droplets and ice crystals in the 200_2 run.

deposited onto ice crystals, increases. This is done by stealing water vapor, which is supposed to be condensed onto droplets, from droplets in an air parcel. As ICNC / CDNC increases in a situation where qsi < qv < qsw, the number of ice crystals, which absorb water vapor, increases per a droplet; here, water vapor absorbed by ice crystals includes that which is produced by droplet evaporation, and qsi represents water vapor saturation pressure for ice water or ice crystals. Thus, as ICNC / CDNC increases, it is likely that the portion of water vapor, which is deposited onto ice crystals in an air parcel, increases, as shown in Lee et al. (2021). This is aided by the higher capacitance of ice crystals compared to that of droplets (Pruppacher and Klett, 1978). Figure 7 shows the time series of the averaged supersaturation over grid points where deposition occurs in the presence of both droplets and ice crystals in the 200_2 run. Figure 7 indicates that, on average, supersaturation occurs for both droplets and ice crystals over those grid points. Hence, on average, the above-described situation of qv > qsw is applicable to deposition when droplets and ice crystals coexist in the 200_2 run.

ICNCavg / CDNCavg is 0.22 in the control run (i.e., the 200_2 run) for the polar case and 0.019 in the control run for the midlatitude case, which is described in Lee et al. (2021). Henceforth, the control run for the midlatitude case is referred to as the control-midlatitude run. ICNCavg / CDNCavg is ∼ 1 order of magnitude higher for the polar case than for the midlatitude case. This is despite the fact that the ratio of the initial number concentration of aerosols acting as INPs to that of those acting as CCN is identical between the 200_2 and control-midlatitude runs. In addition, identical models, model setups (e.g., in terms of vertical resolutions) and sources of reanalysis data are

used between the 200_2 and control-midlatitude runs. How-ever, there are differences in the environmental conditions (e.g., temperature), cloud macrophysical variables (such as cloud top height) and horizontal resolutions between the runs. Here, while taking these similarities and differences into account, we hypothesize that the significant differences in ICNCavg / CDNCavg between runs are mainly due to the fact that ice nucleation strongly depends on air temperature (Prappucher and Klett, 1978). When supercooling is stronger, in general, more ice crystals are nucleated for a given group of aerosols acting as INPs. The average air temperature immediately below the cloud base over the simulation period is $-16,$°C in the 200_2 run and -5°C in the control-midlatitude run. The average air temperature immediately above the cloud top is -33°C in the 200_2 run and -15°C in the control-midlatitude run. Hence, supercooling is greater, and this contributes to the higher ICNCavg / CDNCavg in the polar case than in the midlatitude case. The higher ICNCavg / CDNCavg is likely to induce a greater portion of water vapor to be deposited onto ice crystals in the polar case than in the midlatitude case. It is hypothesized that this, in turn, enables IWC / LWC in the 200_2 run to be 1 order of magnitude greater than that in the control-midlatitude run or in the midlatitude case. Much higher IWC than LWC, which results in a much higher IWC / LWC in the polar case than in the midlatitude case, in the 200_2 run overcomes lower LWC in the 200_2 run than in the 200_0 run, which leads to the greater total cloud mass in the 200_2 run than in the 200_0 run (Fig. 4 and Table 2). However, IWC with a magnitude which is similar to the magnitude of LWC, which results in a much lower IWC / LWC in the midlatitude case than in the polar case, in the midlatitude case is not able to overcome lower LWC in the midlatitude case than in the midlatitude warm clouds, which leads to the greater total cloud mass in the midlatitude warm clouds than in the midlatitude case; here, the midlatitude warm clouds are generated by removing ice processes in the midlatitude case. This means that, in association with higher ICNC / CDNC and IWC / LWC, ice processes enhance the total cloud mass for the polar case as compared to that for the polar warm-cloud counterpart. However, in the midlatitude case, in association with lower ICNC / CDNC and IWC / LWC, ice processes reduce the total cloud mass as compared to that for the midlatitude warm-cloud counterpart.

3.1.4 Role of ICNC / CDNC

To test the hypothesis above about the role of ICNC / CDNC in the above-described differences between the polar and midlatitude cases, the 200_2 run is repeated by reducing ICNCavg / CDNCavg by a factor of 10. This is done by reducing the concentration of aerosols acting as INPs but not those acting as CCN in a way that ICNCavg / CDNCavg is lower by a factor of 10 in the repeated run than in the 200_2 run. In this way, this repeated run has ICNCavg / CDNCavg
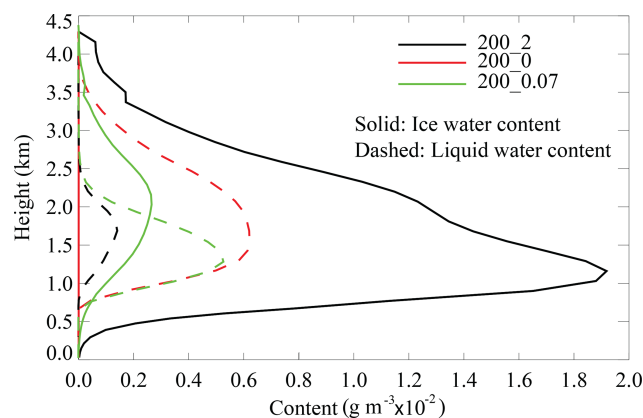

Figure 8. The vertical distributions of the time- and domain-averaged IWC and LWC in the 200_2, 200_0 and 200_0.07 runs.

that is of the same order of magnitude as that in the control-midlatitude run. This repeated run is referred to as the 200_0.07 run. As shown in Fig. 8 and Table 2, the 200_0.07 run shows a much lower deposition rate and IWC than the 200_2 run does. However, as we move from the 200_2 run to the 200_0.07 run, the time- and domain-averaged condensation rate and LWC increase (Fig. 8 and Table 2). This is because a reduction in deposition increases the amount of water vapor, which is not consumed by deposition but is available for condensation. Associated with this, in the 200_0.07 run, the time- and domain-averaged deposition rate and IWC become similar to the average condensation rate and LWC, respectively (Fig. 8 and Table 2). Hence, IWC / LWC is reduced from 26.28 in the 200_2 run to 1.05 in the 200_0.07 run as ICNCavg / CDNCavg is reduced from the 200_2 run to the 200_0.07 run. Here, IWC / LWC in the 200_0.07 run is similar to that in the midlatitude-control run, which demonstrates that the difference in ICNC / CDNC is able to explain the difference in IWC / LWC between the polar and midlatitude cases. It is notable that the reduction in deposition is dominant over the increase in condensation with the decrease in ICNCavg / CDNCavg. Hence, the sum of the condensation and deposition rates and WC are reduced from the 200_2 run to the 200_0.07 run. That the sum of the condensation and deposition rates and WC are reduced in such a way that the sum and WC in the mixed-phase clouds in the 200_0.07 run are lower than the condensation rate and LWC, respectively, in the warm clouds in the 200_0 run is also notable (Fig. 8 and Table 2). This is similar to the situation in the midlatitude case and thus demonstrates that the different relation between the mixed-phase and warm clouds can be associated with the difference in ICNC / CDNC between the polar and midlatitude cases.

The rate of the sedimentation of ice crystals at the cloud base decreases as ICNCavg / CDNCavg decreases between the 200_2 and 200_0.07 runs, mainly due to the reduction in the ice crystal mass (Table 2). The rate of droplet sedimen-

tation at the cloud base increases as ICNCavg / CDNCavg decreases, mainly due to increases in the droplet mass and size in association with the increases in LWC (Table 2). The entrainment rate at the cloud top decreases as ICNCavg / CDNCavg decreases (Table 2). It is found that those changes in the average rates of the droplet and ice crystal sedimentation over the cloud base and simulation period are ∼ 4 to 5 orders of magnitude smaller than those in the average integrated condensation and deposition rates between the 200_2 and 200_0.07 runs (Table 2). The entrainment tends to reduce the total cloud mass or WC less with the decreasing ICNCavg / CDNCavg. Hence, changes in the entrainment counter the decrease in WC with the decreasing ICNCavg / CDNCavg between the 200_2 and 200_0.07 runs. Here, we see that changes in the entrainment are not factors that lead to the increase in LWC; the decrease in IWC; and, eventually, the decrease in WC with the decreasing ICNCavg / CDNCavg. The analysis of the sedimentation and entrainment excludes them from factors inducing the above-described differences between the 200_2 and 200_0.07 runs. Instead, this analysis grants confidence in the fact that deposition and condensation, which are strongly dependent on ICNC / CDNC, are the main factors inducing those differences.

3.2 Aerosol–cloud interactions

Comparisons between the 200_2 and 2000_20 runs show that, with the increasing concentration in aerosols acting as CCN and those as acting INPs, IWC increases, but LWC decreases in the polar case (Fig. 9 and Table 2). These decreases in LWC are negligible as compared to the increases in IWC. Hence, the increases in IWC outweigh the decreases in LWC, leading to aerosol-induced increases in WC (Fig. 9 and Table 2). To identify roles of specific types of aerosols in these aerosol-induced changes, comparisons not only between the 200_2 and 200_20 runs but also between the 200_2 and 2000_2 runs are performed. Comparisons between the 200_2 and 200_20 runs show that the increasing concentration of aerosols acting as INPs induces increases in IWC but decreases in LWC (Fig. 9 and Table 2). The magnitudes of these increases and decreases are similar to those between the 200_2 and 2000_20 runs (Fig. 9 and Table 2). However, comparisons between the 200_2 and 2000_2 runs show that the increasing concentration of aerosols acting as CCN induces negligible changes in either IWC or LWC. Thus, CCN-induced changes in the total cloud mass are negligible, although the increasing concentration of aerosols acting as CCN induces a slight decrease in IWC and a slight increase in LWC (Fig. 9 and Table 2). This demonstrates that INPs plays a much more important role than CCN when it comes to the response of the total cloud mass to increasing aerosol concentrations. However, in the midlatitude case, the increasing concentration of aerosols acting as CCN generates
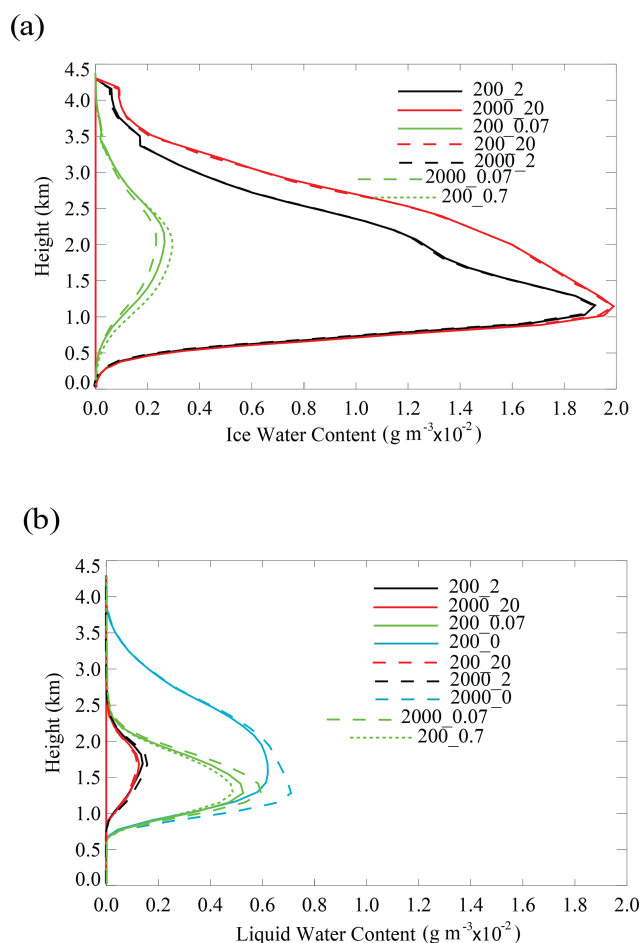
(a)

(b)

Figure 9. (a) The vertical distributions of the time- and domain-averaged IWC in the 200_2, 2000_20, 200_0.07, 200_20, 2000_2, 2000_0.07 and 200_0.7 runs. (b) The vertical distributions of the time- and domain-averaged LWC in the 200_0 and 2000_0 runs, as well as in all the runs shown in panel (a).

changes in the mass as significantly as the increasing concentration of aerosols acting as INPs does.

To identify roles played by ice processes in aerosol-cloud interactions, a pair of the 200_0 and 2000_0 runs are analyzed and compared to the previous four standard simulations (i.e., the 200_2, 200_20, 2000_2 and 2000_20 runs). The CCN-induced increases in LWC in those noice runs are much greater than the CCN-induced changes in WC in the 200_2 and 2000_2 runs (Fig. 9 and Table 2). However, these CCN-induced increases in LWC in the noice runs are smaller than the INP-induced increases in WC in the 200_2 and 200_20 runs (Fig. 9 and Table 2). This is different from the midlatitude case where changes in the total cloud mass, whether they are induced by the increasing concentration of aerosols acting as CCN or INP, in the mixed-phase clouds are much lower than those CCN-induced changes in the warm clouds.

3.2.1 Deposition, condensation, sedimentation and entrainment

The CCN-induced increases in condensation rates and decreases in deposition rates are negligible. This leads to the negligible CCN-induced increases in LWC and the negligible decreases in IWC between the 200_2 and 2000_2 runs (Fig. 9 and Table 2). However, between the 200_2 and 200_20 runs, the significant INP-induced increases are in the deposition rate, leading to the significant INP-induced increases in IWC (Fig. 9 and Table 2). Between the 200_2 and 200_20 runs, INP-induced decreases in condensation rate are negligible, leading to the negligible INP-induced decreases in LWC as compared to the INP-induced increases in deposition rate and IWC (Fig. 9 and Table 2). With the increasing concentration of aerosols acting as INPs from the 200_2 run to the 200_20 run, the sedimentation of ice crystals at the cloud base decreases (Table 2). This is mainly due to decreases in the size of ice crystals in association with increases in INPs and the resultant increases in ICNC. In Fig. 10a, we see that the number concentration of ice crystals with diameters smaller and larger than ~ 40 micron increases and decreases, respectively, as we move from the 200_2 run to the 200_20 run, which indicates a shift in the sizes of ice crystals to smaller ones. From the 200_2 run to the 200_20 run, the sedimentation of droplets at the cloud base decreases, as shown in Table 2, mainly due to decreases in LWC. Figure 10b shows that the number concentration of drops decreases throughout almost all parts of the size range from the 200_2 run to the 200_20 run, which indicates a negligible shift in the drop size but a reduction in LWC. It is found that changes in the average rates of the droplet and ice crystal sedimentation over the cloud base and simulation period are ~ 3 to 4 orders of magnitude smaller than those in the average integrated condensation and deposition rates between the 200_2 and 200_20 runs (Table 2). From the 200_2 run to the 200_20 run, the entrainment at the cloud top increases (Table 2). Hence, the entrainment reduces WC less in the 200_2 run than in the 200_20 run. Here, we see that changes in entrainment and the sedimentation are not factors that we have to focus on to explain the changes in LWC, IWC and WC between the 200_2 and 200_20 runs.

In the warm clouds in the 200_0 and 2000_0 runs, the CCN-induced increases in condensation rate occur, leading to those in LWC (Fig. 9 and Table 2). However, the CCN-induced increases in condensation rate in the warm clouds associated with the polar case are lower than the INP-induced increases in deposition rate in the polar case (Table 2). This contributes to smaller aerosol-induced changes in the total cloud mass in the polar warm clouds than in the polar mixed-phase clouds. The sedimentation of droplets at the cloud base decreases and the entrainment at the cloud top increases from the 200_0 run to the 2000_0 run (Table 2). The increasing concentration of aerosols acting as CCN induces increases in CDNC and decreases in the droplet size,
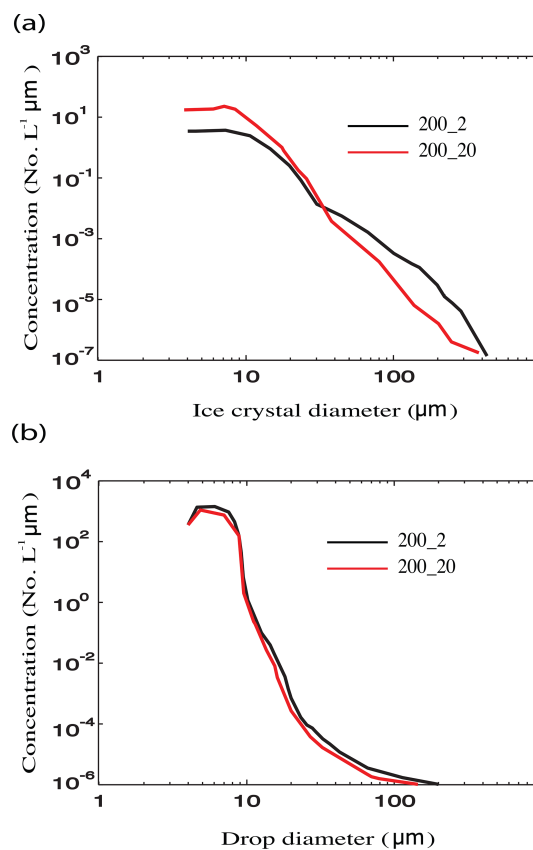
(a)

(b)

Figure 10. The average size distributions of **(a)** ice crystals over grid points with non-zero IWC and the simulation period and **(b)** drops over grid points with non-zero LWC and the simulation period.

leading to the reduction in the droplet sedimentation from the 200_0 run to 2000_0 run. The entrainment counters the CCN-induced increases in LWC from the 200_0 run to the 2000_0 run. Hence, the entrainment is not a factor which induces the CCN-induced increases in LWC between the 200_0 and 2000_0 runs. As seen in Table 2, the changes in the sedimentation rate are ~ 3 orders of magnitude smaller than those in the integrated condensation rate between the 200_0 and 2000_0 runs. Hence, it is not the sedimentation but rather the condensation that we have to look at to explain changes in LWC or WC between the 200_0 and 2000_0 runs.

3.2.2 Understanding differences between the polar and midlatitude cases

Roughly speaking, the CCN-induced changes in LWC via CCN-induced changes in the autoconversion of droplets are proportional to LWC that changing CCN affect, and INP-induced changes in IWC via INP-induced changes in the autoconversion of ice crystals are proportional to IWC that changing INPs affect (e.g., Dudhia, 1989; Murakami, 1990; Liu and Daum, 2004; Morrison et al., 2005, 2009, 2012; Lim

and Hong, 2010; Mansell et al. 2010; Kogan, 2013; Lee and Baik, 2017). This is for given environmental conditions (e.g., temperature and humidity) and given CCN- or INP-induced changes in microphysical factors such as the sizes and number concentrations of droplets or ice crystals. Hence, in the polar case, with a much lower LWC compared to IWC, the changing concentration of aerosols acting as CCN is likely to induce smaller changes in the given LWC via CCN impacts on the droplet autoconversion. This is as compared to changes in the given IWC, which are induced by the changing concentration of aerosols acting as INPs and, thus, the changing ice crystal autoconversion.

The smaller changes in the given LWC are related to changes in CDNC. These changes in CDNC are initiated by those in droplet autoconversion. The larger changes in the given IWC are related to changes in ICNC. These changes in ICNC are initiated by those in ice crystal autoconversion. Changes in integrated droplet surface area, which are induced by those in CDNC, initiate those in the given LWC. Changes in integrated ice crystal surface area, which are induced by those in ICNC, initiate those in the given IWC. Remember that condensation occurs on the droplet surface, and, thus, droplets act as a source of condensation; on the other hand, deposition occurs on the ice crystal surface, and, thus, ice crystals act as a source of deposition. Hence, those changes in CDNC and the associated integrated droplet surface area can lead to changes in condensation and, thus, to feedbacks between condensation and updrafts, while those changes in ICNC and the associated integrated ice crystal surface area can lead to changes in deposition and, thus, to feedbacks between deposition and updrafts. The smaller CCN-induced changes in LWC involve changes in CDNC and associated smaller changes in condensation and in the feedbacks between condensation and updrafts in the polar case. This is as compared to changes in deposition and in feedbacks between deposition and updrafts, which are associated with the INP-induced changes in ICNC and the related larger INP-induced changes in IWC in the polar case. The smaller CCN-induced changes in LWC involve smaller changes in water vapor that is consumed by droplets in the polar case. The larger INP-induced changes in IWC involve larger changes in water vapor that is consumed by ice crystals in the polar case. This leaves the smaller CCN-induced changes in the amount of water vapor available for deposition, which induce the smaller CCN-induced changes in IWC in the polar case. This is as compared to the INP-induced changes in the amount of water vapor which is available for condensation and associated changes in LWC in the polar case.

The lower LWC in the polar warm clouds compared to the IWC in the polar case contributes to the greater INP-induced changes in IWC compared to the CCN-induced changes in LWC in the polar warm clouds. The lower LWC in the polar case compared to that in the polar warm clouds contributes to the greater CCN-induced changes in LWC in the polar

warm clouds compared to those in LWC and the subsequent changes in IWC in the polar case.

In contrast to the situation in the polar case, in the midlatitude case, remember that a given LWC is of the same order of magnitude as IWC. Hence, the CCN-induced changes in LWC and the subsequent changes in IWC are similar to the INP-induced changes in IWC and the subsequent changes in LWC. The greater LWC in the midlatitude warm cloud compared to both LWC and IWC in the midlatitude case contributes to the greater CCN-induced changes in LWC in the midlatitude warm cloud. This is as compared to either the CCN-induced changes in LWC and the subsequent changes in IWC or the INP-induced changes in IWC and the subsequent changes in LWC in the midlatitude case.

In this section, to confirm the above-described mechanisms, which explain different aerosol–cloud interactions between the polar and midlatitude cases, the 200_0.07 run is repeated by increasing INPs by a factor of 10 in the PBL at the first time step. This repeated run is referred to as the 200_0.7 run. Then, the 200_0.07 run is repeated again by increasing the CCN by a factor of 10 in the PBL at the first time step. This repeated run is referred to as the 2000_0.07 run. These repeated runs are to see the response of IWC and LWC to the increasing concentration of aerosols acting as INPs and CCN. This is when IWC and LWC are of the same order of magnitude and lower in mixed-phase clouds than LWC in the warm-cloud counterpart, as in the 200_0.07 run and midlatitude case. Comparisons between the 200_0.07, 200_0.7 and 2000_0.07 runs show that the INP-induced changes in IWC and LWC are similar to the CCN-induced changes in IWC and LWC, respectively, as in the midlatitude case (Fig. 9 and Table 2). These comparisons also show that the CCN-induced changes in LWC in the polar warm cloud are greater (Fig. 9 and Table 2). This is as compared to either the CCN-induced changes in LWC and the subsequent changes in IWC between the 200_0.07 and 2000_0.07 runs or the INP-induced changes in IWC and the subsequent changes in LWC between the 200_0.07 and 200_0.7 runs (Fig. 9 and Table 2). These comparisons demonstrate that differences in ICNC / CDNC play a critical role in differences in aerosol–cloud interactions between the polar and midlatitude cases, considering the fact that differences in ICNC / CDNC between the 200_2 and 200_0.07 runs are of the same order of magnitude as those between the cases.

3.3 Radiation

Studies (e.g., Ovchinnikov et al., 2011; Possner et al., 2017; Solomon et al., 2018) have focused on radiative cooling and subsequent changes in stability and dynamics as a primary driver for the development of mixed-phase stratocumulus clouds and for aerosol-induced changes in LWC and IWC in those clouds. Motivated by these studies, to isolate the role of radiative processes in cloud development and aerosol impacts on LWC and IWC, all of the simulations above are re-

peated by turning off radiative processes. In these repeated runs, radiative fluxes over the whole domain and simulation period are zero. The basic summary of results from these repeated runs is given in Table 3. As seen in comparisons between Tables 2 and 3, in this study, the qualitative nature of the results – which are mainly about differences in IWC / LWC, the relative importance of the impacts of INPs on IWC and LWC as compared to the impacts of CCN, and how warm and mixed-phase clouds are related between the polar and midlatitude cases – does not vary with whether radiative processes exist or not. This demonstrates that ICNC, CDNC, deposition and condensation (but not radiative processes) drive the results in this study.

4 Discussion

4.1 Examination of the role of ICNC / CDNC in IWC / LWC in the 200_2, 2000_20, 2000_2, 200_20, 200_0.07, 2000_0.07 and 200_0.7 runs

So far, comparisons between the set of the 200_2, 2000_20, 2000_2 and 200_20 runs for the polar case and the other set of the 200_0.07, 2000_0.07 and 200_0.7 runs, which represents the midlatitude case, have mainly been utilized to understand the role of ICNC / CDNC. However, even when it comes to all the runs in both the sets, differences in ICNCavg / CDNCavg and IWC / LWC are shown among them (Tables 1 and 2). For a more robust examination of, in particular, the role of ICNC / CDNC in IWC / LWC, which is basically about the increase and/or decrease in ICNC / CDNC inducing the increase and/or decrease in IWC / LWC, as identified from the comparison between the 200_2 and 200_0.07 runs in Sect. 3.1.4, all the runs in the sets are utilized by ordering them as shown in Table 4. This ordering is done in such a way that, as we move from the first run in the first row to the last run in the last row of Table 4, ICNCavg / CDNCavg increases. Overall, with increasing ICNCavg / CDNCavg, IWC / LWC increases in Table 4, as also seen in Fig. 11, which shows IWC / LWC as a function of ICNCavg / CDNCavg based on Table 4. This is despite the fact that the increase in IWC / LWC is highly nonlinear in terms of the increase in ICNCavg / CDNCavg, as seen in the percentage increases, and a decrease in IWC / LWC is seen with an increase in ICNCavg / CDNCavg from the 2000_20 run to the 200_2 run (Table 4 and Fig. 11); this high-degree nonlinearity in the increase in IWC / LWC is associated with the fact that interactions between cloud microphysical, thermodynamic and dynamic processes are well known to be highly nonlinear. Hence, overall, findings regarding the role of ICNC / CDNC in IWC / LWC from the comparison between the 200_2 and 200_0.07 runs are applicable to all the runs in the sets, except for the role between the 2000_20 and 200_2 runs. Here, it is notable that the percentage difference in ICNCavg / CDNCavg is ∼ 9 % between the 2000_20 and 200_2 runs, and this is the smallest among those differences
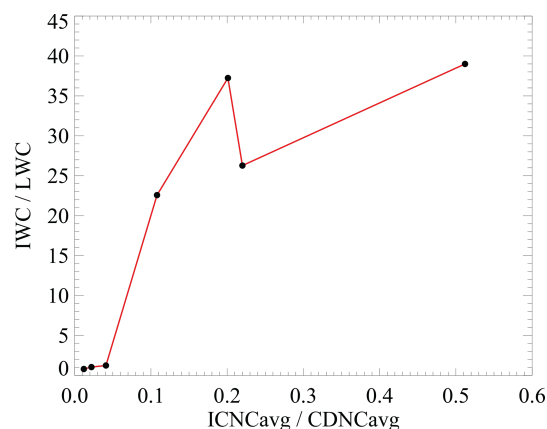

Figure 11. IWC / LWC as a function of ICNCavg / CDNCavg based on Table 4.

in Table 4. The other differences are larger than 80 %. Hence, the percentage difference in ICNCavg / CDNCavg for a pair of the 2000_20 and 200_2 runs is at least ∼ 1 order of magnitude smaller than that for the other pairs of runs in Table 4. This means that findings from the comparison between the 200_2 and 200_0.07 runs are not suitable to explain the variation in IWC / LWC among clouds when the variation in ICNC / CDNC is relatively insignificant. According to Table 4, it seems that the variation in ICNC / CDNC should be greater than a critical value above which those findings are useful in accounting for the IWC / LWC variation among clouds.

The high-degree nonlinearity in the variation in IWC / LWC is epitomized by the 1706 % increase in IWC / LWC in relation to the 163 % increase in ICNCavg / CDNCavg from the 200_0.7 run to the 2000_2 run. This 1706 % percent increase in IWC / LWC is induced by increases in the initial number concentrations of both CCN and INPs between the runs (Table 1). In other transitions from a simulation in a row to that in the next row in Table 4, there are decreases in the initial number concentrations of both CCN and INPs, or there is a change in the initial number condensation of either CCN or INPs. When the initial concentration of either CCN or INPs changes in the transition, an increase of less than 100 % in IWC / LWC is shown. The decreases in the initial number concentrations of both CCN and INPs, which are from the 2000_20 run to the 200_2 run, result in the decrease in IWC / LWC. Hence, depending on how the initial number concentrations of CCN and INPs change, the magnitude and sign of the change in IWC / LWC can vary substantially.

Table 4. ICNCavg / CDNCavg and IWC / LWC in the simulations that are discussed in Sect. 4.1. The percentage increases or decreases in ICNCavg / CDNCavg and IWC / LWC, as shown in the ith, row are $\frac{(\text{ICNCavg / CDNCavg})_i - (\text{ICNCavg / CDNCavg})_{i-1}}{(\text{ICNCavg / CDNCavg})_{i-1}} \times 100\,(\%)$ and $\frac{(\text{IWC / LWC})_i - (\text{IWC / LWC})_{i-1}}{(\text{IWC / LWC})_{i-1}} \times 100\,(\%)$, respectively. Here, $(\text{ICNCavg / CDNCavg})_i$ and $(\text{IWC / LWC})_i$ represent ICNCavg / CDNCavg and IWC / LWC in the ith row, respectively.

Simulations	ICNCavg / CDNCavg	Percentage increases (+) or decrease (−) in ICNCavg / CDNCavg	IWC / LWC	Percentage increases (+) or decrease (−) in IWC / LWC
2000_0.07	0.012		0.81	
200_0.07	0.022	+83.33 %	1.05	+29.6 %
200_0.7	0.041	+86.36 %	1.25	+19.0 %
2000_2	0.108	+163.4 %	22.58	+1706.4 %
2000_20	0.201	+86.1 %	37.24	+64.9 %
200_2	0.220	+9.4 %	26.28	−29.4 %
200_20	0.512	+132.7 %	39.00	+48.4 %

4.2 Role of a given ICNC / CDNC in IWC / LWC for different concentrations of aerosols acting as INPs and CCN

Simulations which are compared in Sect. 4.1 and shown in Table 4 not only have different ICNCavg / CDNCavg values but also have different number concentrations of aerosols acting as CCN and INPs at the first time step (Table 1). To better isolate the role of ICNC / CDNC in IWC / LWC in particular, we need to show that results in Sect. 4.1 are valid regardless of the variation in the number concentration of aerosols. For this, we focus on the 200_2 and 200_0.07 runs since the primary understanding of the role of ICNC / CDNC in IWC / LWC comes from the comparison between these runs, as described in Sect. 3.1.4. To fulfill the need, each of these runs are repeated by varying the number concentration of aerosols acting as CCN and INPs in such a way that ICNCavg / CDNCavg does not vary (Tables 1 and 5). The 4000_45 and 13_0.1 runs are the repeated 200_2 run, and the 4000_1.8 and 12_0.0035 runs are the repeated 200_0.07 run (Tables 1 and 5). The set of the 200_2, 4000_45 and 13_0.1 runs is referred to as the polar set, and that of the 200_0.07, 4000_1.8 and 12_0.0035 runs is referred to as the midlatitude set in this section. Among the three runs in each of the sets, less than 4 % variation in IWC / LWC is shown (Table 5). This variation of less than 4 % is so small that the start contrast in IWC / LWC between the 200_2 and 200_0.07 runs, as discussed in Sect. 3.1.4, is also shown between the polar and midlatitude sets (Table 5). Hence, the role of the difference in a given ICNC / CDNC in the difference in IWC / LWC between the 200_2 and 200_0.07 runs, as described in Sect. 3.1.4, is considered to be robust in relation to the varying concentration of aerosols.

Table 5. ICNCavg / CDNCavg and IWC / LWC in the simulations that are discussed in Sect. 4.2. The percentage increases or decreases in IWC / LWC in the 4000_45 run or in the 13_0.1 run are $\frac{(\text{IWC/LWC})_{4000\_45\text{ or }13\_0.1} - (\text{IWC/LWC})_{200\_2}}{(\text{IWC/LWC})_{200\_2}} \times 100\,(\%)$. Here, $(\text{IWC/LWC})_{4000\_45\text{ or }13\_01}$ represents IWC / LWC in the 4000_45 run or the 13_01 run, while $(\text{IWC / LWC})_{200\_2}$ represents IWC / LWC in the 200_2 run. The percentage increases or decreases in IWC / LWC in the 4000_1.8 run or the 12_0.0035 run are $\frac{(\text{IWC/LWC})_{4000\_1.8\_fac10\text{ or }12\_0.0035\_fac10} - (\text{IWC/LWC})_{200\_2\_fac10}}{(\text{IWC/LWC})_{200\_2\_fac10}} \times 100\,(\%)$. Here, $(\text{IWC / LWC})_{4000\_1.8\text{ or }12\_0.0035}$ represents IWC / LWC in the 4000_1.8 run or the 12_0.0035 run, while $(\text{IWC / LWC})_{200\_0.07}$ represents IWC / LWC in the 200_0.07 run.

Simulations	ICNCavg / CDNCavg	IWC /LWC	Percentage increases (+) or decrease (−) in IWC / LWC
Polar case			
200_2	0.220	26.28	
4000_45	0.220	27.25	+3.7 %
13_0.1	0.220	25.62	−2.5 %
Representing midlatitude case			
200_0.07	0.022	1.05	
4000_1.8	0.022	1.09	+3.8 %
12_0.0035	0.022	1.02	−2.9 %

4.3 Role of environmental factors, sedimentation, aerosol sources and advection

This study employs ICNC / CDNC as an important factor which differentiates IWC / LWC and interactions among clouds, aerosols and ice processes in the polar case from those in the midlatitude case. However, this does not mean that no other potential factors which can explain the variation in IWC / LWC and interactions among clouds, aerosols and

ice processes between different clouds exist. For example, differences in environmental factors (e.g., stability and wind shear) between those different clouds can have an impact on the variation. Particularly, differences in stability and wind shear can initiate those in the dynamic development of turbulence. Then, this subsequently induces differences in the microphysical and thermodynamic development of clouds; IWC / LWC; and interactions among clouds, aerosols and ice processes. Hence, factors such as stability and wind shear can have different orders of procedures, which involve dynamics, thermodynamics and microphysics, than ICNC / CDNC in terms of differentiation between different clouds. Thus, different mechanisms controlling the differentiation can be expected with regard to factors such as stability and wind shear as compared to ICNC / CDNC. The examination of these different mechanisms among stability, wind shear and ICNC / CDNC deserves future study for a more comprehensive understanding of the differentiation or for a more fully established general principle explaining the differentiation.

Another point to make is that the cases in this study have weak precipitation and an associated weak sedimentation of ice crystals and droplets. In mixed-phase clouds with strong precipitation and sedimentation, they can play roles that are as important as in-cloud latent-heat processes in IWC / LWC and in interactions among clouds, aerosols and ice processes. In those clouds with strong precipitation, the sedimentation can take part in the interplay between ICNC / CDNC and latent-heat processes by affecting cloud mass and associated ICNC and CDNC significantly and can play a role in the differentiation of IWC / LWC and interactions among clouds, aerosols and ice processes when it comes to different cases of mixed-phase clouds. Here, for more of a generalization of the results as a means to develop the more fully established general principle, this potential role of sedimentation needs to be investigated by performing more case studies involving cases with strong precipitation in the future.

It should be emphasized that, although this study mentions air temperature as a factor that affects ICNC / CDNC, ICNC / CDNC can be affected by other factors such as sources of aerosols acting as INPs and those acting as CCN and/or the advection of those aerosols. Hence, even for cloud systems that develop with a similar air temperature condition, for example, when those systems are affected by different sources of aerosols and/or their different advection, they are likely to have different ICNC / CDNC and IWC / LWC, as well as a different relative importance of the impacts of INPs on IWC and LWC as compared to those impacts of CCN, along with different relations between warm and mixed-phase clouds. Regarding factors which affect ICNC / CDNC, such as the sources and advection of aerosols together with temperature, it should be noted that, while this study utilizes differences in temperature among those factors to identify cases exhibiting significant disparities in ICNC / CDNC, its primary objective does not lie in the role of temperature differences in disparities in ICNC / CDNC but rather in comprehending the inherent role of ICNC / CDNC variations themselves in the discrepancies observed, for example, in IWC / LWC, across diverse cloud systems.

4.4 Mixing of droplets and ice crystals

The representation of mixed-phase clouds in our study relies on the assumption of homogeneously mixed ice and liquid hydrometeors within the model grid cells, a common approach in many models. However, recent observational studies (e.g., D'Alessandro et al., 2021; Korolev and Milbrandt, 2022; Schima et al., 2022; Coopman and Tan, 2023) have shown that, in reality, mixed-phase clouds often exhibit inhomogeneous distributions of ice and liquid, with distinct pockets or regions of each phase. These observations suggest that the microphysical processes, such as the Wegener–Bergeron–Findeisen process, may be influenced by this inhomogeneity, potentially leading to differences in cloud dynamics and feedbacks compared to what is simulated by models assuming the homogeneous mixing.

While our study, along with the work of Lee et al. (2021), uses a model-based approach that assumes the homogeneous mixing, it is important to acknowledge that this representation may not fully capture the complexity observed in real clouds. The implications of this assumption could affect the accuracy of our simulations, particularly in scenarios where phase transition processes in mixed-phase clouds play a significant role. As such, the results presented should be interpreted with this limitation in mind, and further work incorporating more detailed representations of inhomogeneous hydrometeor distributions may be needed to refine our understanding of mixed-phase cloud processes.

5 Summary and conclusions

In this study, a case of mixed-phase stratiform clouds in a polar area, which is referred to as the polar case, is compared to that in a midlatitude area, which is referred to as the midlatitude case. This is to gain an understanding of how a different ICNC / CDNC plays a role in making differences in cloud properties, aerosol–cloud interactions and impacts of ice processes on them between two representative areas (i.e., polar and midlatitude areas) where mixed-phase stratiform clouds form and develop. Among those cloud properties, this study focuses on IWC / LWC that plays an important role in cloud radiative properties. To gain the understanding efficiently, the polar case is chosen in such a way to show the stark contrast with the midlatitude case in terms of ICNC / CDNC and IWC / LWC. Although such polar cases may be uncommon, the stark contrast provides an opportunity to elucidate mechanisms that control the above-mentioned role of different ICNC / CDNC.

Due to lower air temperature, more ice crystals are nucleated, leading to higher ICNC / CDNC in the polar case than in the midlatitude case. This higher ICNC / CDNC enables

the more efficient deposition of water vapor onto ice crystals in the polar case. This leads to much higher IWC / LWC in the polar case. The more efficient deposition of water vapor onto ice crystals enables the polar mixed-phase clouds to have the greater total cloud mass compared to the polar warm clouds. However, the less efficient deposition of water vapor onto ice crystals causes the midlatitude mixed-phase clouds to have less total cloud mass than the midlatitude warm clouds. With the increasing ICNC / CDNC from the midlatitude case to the polar case, impacts of CCN and INPs on the total cloud mass become less and more important, respectively.

Previous studies on mixed-phase stratocumulus clouds (e.g., Ovchinnikov et al., 2011; Possner et al., 2017; Solomon et al., 2018) have primarily focused on investigating the impacts of cloud top radiative cooling, entrainment and sedimentation of ice particles on these clouds, as well as on their interactions with aerosols. However, there is a scarcity of studies that specifically examine the role of microphysical interactions involving processes such as condensation and deposition, as well as factors like cloud particle concentrations, between ice and liquid particles in mixed-phase stratocumulus clouds and their interactions with aerosols, as considered in this study. Therefore, our study contributes to a more comprehensive understanding of mixed-phase clouds and their intricate interplay with aerosols.

This study suggests that a microphysical factor, which is ICNC / CDNC, can be a simplified and useful tool to understand differences among different systems of stratocumulus clouds in various regions in terms of IWC / LWC and the relative importance of INPs and CCN in aerosol–cloud interactions; thus, this factor contributes to the development of general parameterizations of those clouds in various regions for climate models. This factor can also be a useful tool for a simplified understanding of the different roles of ice processes when mixed-phase clouds are compared to their warm-cloud counterparts in terms of the cloud development and its interactions with aerosols among those different systems. It should be noted that warm clouds have been studied much more than mixed-phase clouds, although mixed-phase clouds play as important a role as warm clouds in the evolution of climate. This study provides preliminary mechanisms which differentiate mixed-phase clouds and their interactions with aerosols from their warm-cloud counterparts and which control the variation in the differentiation in different regions as a way of improving our understanding of mixed-phase clouds. It should be mentioned that the efficient way of developing general parameterizations, which are for climate models and consider all of the warm and mixed-phase clouds in various regions and their interactions with aerosols, can be achieved by just adding those mechanisms to pre-existing parameterizations of much-studied warm clouds instead of developing brand new parameterizations from the scratch.

This study finds that the relation between ICNC / CDNC and IWC / LWC is highly nonlinear. This high nonlinearity is closely linked to how the number concentrations of CCN and INPs and the associated ICNC / CDNC change. For a specific situation where the ICNC / CDNC variation is relatively small and where the number concentrations of both CCN and INPs decrease, the increase in ICNC / CDNC can reduce IWC / LWC, although it is found that, as a whole, the increase in ICNC / CDNC enhances IWC / LWC. Hence, mechanisms identified in this study, especially regarding the use of ICNC / CDNC as a simplified and useful tool to explain differences in IWC / LWC among different cloud systems, are not complete and are entirely general. In addition, results in this study are from only two cases in two specific locations in the midlatitude and Arctic regions, and the need for greater generalizability of the results from this study merits more case studies over more locations in those regions with regard to, for example, the above-mentioned sedimentation intensity, factors (e.g., environmental factors) other than ICNC / CDNC, different sources and advection of aerosols, the magnitude of the variation in ICNC / CDNC, and the way number concentrations of CCN and INPs vary. Hence, findings from this study, particularly about the relations between ICNC / CDNC and IWC / LWC, should be considered to be preliminary ones that can be used to initiate future work to streamline the development of the general parameterizations.

Author contributions. The essential initial ideas were provided by SSL, CHJ and YJY to start this work. The simulation and observation data were analyzed by SSL, CHJ and JG. YZ, JG, MGM and SKS reviewed the results and contributed to their improvement. JC provided support to set up and run additional simulations during the review process.

References

Ackerman, A., Kirkpatrick, M. P., Stevens, D. E., and Toon, O. B.: The impact of humidity above stratiform clouds on indirect aerosol climate forcing, Science, 432, 1014–1017, https://doi.org/10.1038/nature03174, 2004.

Albrecht, B. A.: Aerosols, cloud microphysics, and fractional cloudiness, Science, 245, 1227–1230, https://doi.org/10.1126/science.245.4923.1227, 1989.

Bartosiewicz, Y. and Duponcheel, M.: Large eddy simulation: Application to liquid metal fluid flow and heat transfer, in: Thermal hydraulics aspects of liquid metal cooled nuclear reactors, edited by: Roelofs, F., 1st ed., Woodhead Publishing, Cambridge, UK, 255–278, ISBN 9780081019818, 2018.

Brown, A., Milton, S., Cullen, M., Golding, B., Mitchell, J., and Shelly, A.: Unified modeling and prediction of weather and climate: A 25-year journey, B. Am. Meteor. Soc., 93, 1865–1877, https://doi.org/10.1175/BAMS-D-12-00018.1, 2012 (data available at: https://www.metoffice.gov.uk/about-us/contact, last access: 15 November 2024).

Chen, F. and Dudhia, J.: Coupling an advanced land-surface hydrology model with the Penn State-NCAR MM5 modeling system. Part I: Model description and implementation, Mon. Weather Rev., 129, 569–585, https://doi.org/10.1175/1520-0493(2001)129<0569:CAALSH>2.0.CO;2, 2001.

Choi, Y.-S., Ho, C.-H., Park, C.-E., Storelvmo, T., and Tan, I.: Influence of cloud phase composition on climate feedbacks, J. Geophys. Res., 119, 3687–3700, https://doi.org/10.1002/2013JD020582, 2014.

Choi, Y.-S., Lindzen, R. S., Ho, C.-H., and Kim, J.: Space observations of cold-cloud phase change, P. Natl. Acad. Sci. USA, 107, 11211–11216, https://doi.org/10.1073/pnas.1006241107, 2010.

Chua, X. R. and Ming, Y.: Convective invigoration traced to warm-rain microphysics, Geophys. Res. Lett, 47, e2020GL089134, https://doi.org/10.1029/2020GL089134, 2020.

Coopman, Q. and Tan, I.: Characterization of the spatial distribution of the thermodynamic phase within mixed-phase clouds using satellite observations, Geophys. Res. Lett., 50, e2023GL104977, https://doi.org/10.1029/2023GL104977, 2023.

D'Alessandro, J. J., McFarquhar, G. M., Wu, W., Stith, J. L., Jensen, J. B., and Rauber, R. M.: Characterizing the occurrence and spatial heterogeneity of liquid, ice, and mixed phase low-level clouds over the Southern Ocean using in situ observations acquired during SOCRATES, J. Geophys. Res., 126, e2020JD034482, https://doi.org/10.1029/2020JD034482, 2021.

Dione, C., Lohou, F., Lothon, M., Adler, B., Babić, K., Kalthoff, N., Pedruzo-Bagazgoitia, X., Bezombes, Y., and Gabella, O.: Low-level stratiform clouds and dynamical features observed within the southern West African monsoon, Atmos. Chem. Phys., 19, 8979–8997, https://doi.org/10.5194/acp-19-8979-2019, 2019.

Donovan, D. P.: Ice-cloud effective particle size parameterization based on combined lidar, radar reflectivity, and mean Doppler velocity measurements, J. Geophys. Res., 108, 4573, https://doi.org/10.1029/2003JD003469, 2003.

Donovan, D. P. and van Lammeren, A. C. A. P.: Cloud effective particle size and water content profile retrievals using combined lidar and radar observations: 1. Theory and examples, J. Geophys. Res., 106, 27425–27448, https://doi.org/10.1029/2001JD900243, 2001.

Donovan, D. P., van Lammeren, A. C. A. P., Hogan, R. J., Russchenberg, H. W. J., Apituley, A., Francis, P., Testud, J., Pelon, J., Quante, M., and Goddard, J. W. F.: Cloud effective particle size and water content profile retrievals using combined lidar and radar observations – 2. Comparison with IR radiometer and in situ measurements of ice clouds, J. Geophys. Res, 106, 27449–27464, https://doi.org/10.1029/2001JD900243, 2001.

Dudhia, J.: Nemerical study of convection observed during the winter monsoon Experiment using a mesoscale two-dimensional Model, J. Atmos. Sci., 46, 3077–3107, https://doi.org/10.1175/1520-0469(1989)046<3077:NSOCOD>2.0.CO;2, 1989.

Fan, J., Rosenfeld, D., Zhang, Y., Giangrande, S. E., Li, Z., Machado, L. A. T., Martin, S. T., Yang, Y., Wang, J., and Artaxo, P.: Substantial convection and precipitation enhancements by ultrafine aerosol particles, Science, 359, 411–418, https://doi.org/10.1126/science.aan8461, 2018.

Forster, P., Ramaswamy, V., Artaxo, P., Berntsen, T., Betts, R., Fahey, D. W., Haywood, J., Lean, J., Lowe, D. C., Myhre, G., Nganga, J., Prinn, R., Raga, G., Schulz, M., and van Dorland, R.: Changes in atmospheric constituents and in radiative forcing, in: Climate Change 2007: the physical science basis, edited by: Solomon, S., Qin, D., Manning, M., Chen, Z., Marquis, M., Averyt, K. B., Tignor, M., and Miller, H. L., Contribution of working group I to the Fourth Assessment Report of the Intergovernmental Panel on Climate Change, Cambridge University Press, Cambridge, UK, and New York, NY, USA, 129–234, ISBN 9780521705967, 2007.

Gettelman, A., Liu, X., Barahona, D., Lohmann, U., and Chen, C.: Climate impacts of ice nucleation, J. Geophys. Res., 117, D20201, https://doi.org/10.1029/2012JD017950, 2012.

Gras, J. L.: Southern hemisphere tropospheric aerosol microphysics, J. Geophys. Res., 96, 5345–5356, https://doi.org/10.1029/89JD00429, 1991.

Hahn, C. J. and Warren, S. G.: A gridded climatology of clouds over land (1971–96) and ocean (1954–97) from surface observations worldwide, Numeric Data Package NDP-026E,

ORNL/CDIAC-153, Carbon Dioxide Information Analysis Center (CDIAC), Department of Energy, Oak Ridge, TN, USA, 71 pp., https://doi.org/10.3334/CDIAC/cli.ndp026e, 2007.

Hannak, L., Knippertz, P., Fink, A. H., Kniffka, A., and Pante, G.: Why do global climate models struggle to represent low-level clouds in the West African summer monsoon?, J. Climate, 30, 1665–1687, https://doi.org/10.1175/JCLI-D-16-0451.1, 2017.

Hansen, A., Ament, F., Grützun, V., and Lammert, A.: Model evaluation by a cloud classification based on multi-sensor observations, Geosci. Model Dev. Discuss. [preprint], https://doi.org/10.5194/gmd-2018-259, 2018.

Hartmann, D. L., Ockert-Bell, M. E., and Michelsen, M. L.: The effect of cloud type on earth's energy balance–Global analysis, J. Climate, 5, 1281–1304, https://doi.org/10.1175/1520-0442(1992)005<1281:TEOCTO>2.0.CO;2, 1992.

Hartmann, M., Gong, X., Kecorius, S., van Pinxteren, M., Vogl, T., Welti, A., Wex, H., Zeppenfeld, S., Herrmann, H., Wiedensohler, A., and Stratmann, F.: Terrestrial or marine – indications towards the origin of ice-nucleating particles during melt season in the European Arctic up to 83.7° N, Atmos. Chem. Phys., 21, 11613–11636, https://doi.org/10.5194/acp-21-11613-2021, 2021.

Hogan, R. J., Illingworth, A. J., O'Connor, E. J., Bouniol, D., Brooks, M. E., Delanoë, J., Donovan, D. P., Eastment, J. D., Gaussiat, N., Goddard, J. W. F., Haeffelin, M., Klein Baltink, H., Krasnov, O. A., Pelon, J., Piriou, J.-M., Protat, A., Russchenberg, H. W. J., Seifert, A., Tompkins, A. M., van Zadelhoff, G.-J., Vinit, F., Westbrook, C. D., Willén, U., Wilson, D. R., and Wrench, C. L.: Cloudnet: Evaluation of model clouds using ground-based observations, in: Proceedings of the ECMWF workshop on parametrization of clouds in large-scale models, 13–15 November 2006, European Centre for Medium-Range Weather Forecasts (ECMWF), Reading, UK, 113–130, 2007 (data available at: https://cloudnet.fmi.fi/search/data, last access: 15 November 2024).

Illingworth, A. J., Hogan, R. J., O'Connor, E. J., Bouniol, D., Brooks, M. E., Delanoé, J., Donovan, D. P., Eastment, J. D., Gaussiat, N., Goddard, J. W. F., Haeffelin, M., H. Baltink, K. H., Krasnov, O. A., Pelon, J., Piriou, J.-M., Protat, A., Russchenberg, H. W. J., Seifert, A., Tompkins, A. M., van Zadelhoff, G.-J., Vinit, F., Willén, U., Wilson, D. R., and Wrench, C. L.: Cloudnet – continuous evaluation of cloud profiles in seven operational models using ground-based observations, B. Am. Meteor. Soc., 88, 883–898, https://doi.org/10.1175/BAMS-88-6-883, 2007.

IPCC: Climate Change: The Physical Science Basis, Contribution of Working Group I to the Sixth Assessment Report of the Intergovernmental Panel on Climate Change, edited by: Masson-Delmotte, V., Zhai, P., Pirani, A., Connors, S. L., Péan, C., Berger, S., Caud, N., Chen, Y., Goldfarb, L., Gomis, M. I., Huang, M., Leitzell, K., Lonnoy, E., Matthews, J. B. R., Maycock, T. K., Waterfield, T., Yelekçi, O., Yu, R., and Zhou, B., Cambridge University Press, Cambridge, United Kingdom and New York, NY, USA, https://doi.org/10.1017/9781009157896, 2021.

Jaenicke, R.: Tropospheric aerosols in Aerosol-Cloud-Climate Interactions, edited by: Hobbs, P. V., Academic Press, San Diego, CA, 54, 1–31, https://doi.org/10.1016/S0074-6142(08)60210-7, 1993.

Jiang, H., Feingold, G., and Cotton, W. R: Simulations of aerosol-cloud-dynamical feedbacks resulting from entrainment of aerosol into the marine boundary layer during the Atlantic Stratocumulus Transition Experiment, J. Geophys. Res., 107, 4813, https://doi.org/10.1029/2001JD001502, 2002.

Jung, C. H., Yoon, Y. J., Kang, H. J., Gim, Y., Lee, B. Y., Ström, J., Krejci, R., and Tunved, P.: The seasonal characteristics of cloud condensation nuclei (CCN) in the arctic lower troposphere, Tellus B, 70, 1513291, https://https://doi.org/10.1080/16000889.2018.1513291, 2018.

Khain, A., Pokrovsky, A., Rosenfeld, D., Blahak, U., and Ryzhkoy, A.: The role of CCN in precipitation and hail in a mid-latitude storm as seen in simulations using a spectral (bin) microphysics model in a 2D dynamic frame, Atmos. Res., 99, 129–146, https://doi.org/10.1016/j.atmosres.2010.09.015, 2011.

Khain, A. P., Ovchinnikov, M., Pinsky, M., Pokrovsky, A. and Krugliak, H.: Notes on the state-of-the-art numerical modeling of cloud microphysics, Atmos. Res., 55, 159–224, https://doi.org/10.1016/S0169-8095(00)00064-8, 2000.

Khain, A. P., Phillips, V., Benmoshe, N., and Pokrovsky, A.: The role of small soluble aerosols in the microphysics of deep maritime clouds, J. Atmos. Sci., 69, 2787–2807, https://doi.org/10.1016/j.atmosres.2010.09.015, 2012.

Knippertz, P., Fink, A. H., Schuster, R., Trentmann, J., Schrage, J. M., and Yorke, C.: Ultra-low clouds over the southern West African monsoon region, Geophys. Res. Lett., 38, L21808, https://doi.org/10.1029/2011GL049278, 2011.

Korolev, A. and Milbrandt, J.: How are mixed-phase clouds mixed?, Geophys. Res. Lett., 49, e2022GL099578, https://doi.org/10.1029/2022GL099578, 2022.

Kogan, Y.: A cumulus cloud microphysics parameterization for cloud-resolving models, J. Atmos. Sci., 70, 1423–1436, https://https://doi.org/10.1175/JAS-D-12-0183.1, 2013.

Koop, T., Luo, B. P., Tsias, A., and Peter, T.: Water activity as the determinant for homogeneous ice nucleation in aqueous solutions, Nature, 406, 611–614, https://doi.org/10.1038/35020537, 2000.

Lee, H. and Baik, J.-J.: A physically based autoconversion parameterization, J. Atmos. Sci., 74, 1599–1616, https://doi.org/10.1175/JAS-D-16-0207.1, 2017.

Lee S. S., Penner, J. E., and Saleeby, S. M.: Aerosol effects on liquid-water path of thin stratocumulus clouds, J. Geophys. Res., 114, D07204, https://doi.org/10.1029/2008JD010513, 2009.

Lee, S. S., Ha, K.-J., Manoj, M. G., Kamruzzaman, M., Kim, H., Utsumi, N., Zheng, Y., Kim, B.-G., Jung, C. H., Um, J., Guo, J., Choi, K. O., and Kim, G.-U.: Midlatitude mixed-phase stratocumulus clouds and their interactions with aerosols: how ice processes affect microphysical, dynamic, and thermodynamic development in those clouds and interactions?, Atmos. Chem. Phys., 21, 16843–16868, https://doi.org/10.5194/acp-21-16843-2021, 2021.

Li, J., Carlson, B. E., Yung, Y. L., Lv, D., Hansen, J., Penner, J. E., Liao, H., Ramaswamy, V., Kahn, R. A., Zhang, P., Dubovik, O., Ding, A., Lacis, A. A., Zhang, L., and Dong, Y.: Scattering and absorbing aerosols in the climate system, Nat. Rev. Earth Environ., 3, 363–379, https://doi.org/10.1038/s43017-022-00296-7, 2022.

Lilly, D. K.: The representation of small scale turbulence in numerical simulation experiments, Proc. Ibm

Sci. Comput. Symp. Environ. Sci., 320–1951, 195–210, https://doi.org/10.5065/D62R3PMM, 1967.

Lim, K.-S. S. and Hong, S.-Y.: Development of an effective double-moment cloud microphysics scheme with prognostic cloud condensation nuclei (CCN) for weather and climate models, Mon. Weather Rev., 138, 1587–1612, https://doi.org/10.1175/2009MWR2968.1, 2010.

Liu, Y. and Daum, P. H.: Parameterization of the autoconversion. Part I: Analytical formulation of the Kessler-type parameterizations, J. Atmos. Sci., 61, 1539–1548, https://doi.org/10.1175/1520-0469(2004)061<1539:POTAPI>2.0.CO;2, 2004.

Lohmann, U. and Diehl, K.: Sensitivity studies of the importance of dust ice nuclei for theindirect aerosol effect on stratiform mixed-phase clouds, J. Atmos. Sci., 63, 968–982, https://doi.org/10.1175/JAS3662.1, 2006.

Mansell, E. R., Ziegler, C. L., and Bruning, E. C., Simulated electrification of a small thunderstorm with two-moment bulk microphysics, J. Atmos. Sci., 67, 171–194, https://doi.org/10.1175/2009JAS2965.1., 2010.

Mlawer, E. J., Taubman, S. J., Brown, P. D., Iacono, M. J., and Clough, S. A.: RRTM, a validated correlated-k model for the longwave, J. Geophys. Res., 102, 16663–1668, https://doi.org/10.1029/97JD00237,1997.

Moeng, C.-H., Sullivan, P. P., and Stevens, B.: Including radiative effects in an entrainment rate formula for buoyancy-driven PBLs, J. Atmos. Sci., 56, 1031–1049, https://doi.org/10.1175/1520-0469(1999)056<1031:IREIAE>2.0.CO;2, 1999.

Möhler, O., Field, P. R., Connolly, P., Benz, S., Saathoff, H., Schnaiter, M., Wagner, R., Cotton, R., Krämer, M., Mangold, A., and Heymsfield, A. J.: Efficiency of the deposition mode ice nucleation on mineral dust particles, Atmos. Chem. Phys., 6, 3007–3021, https://doi.org/10.5194/acp-6-3007-2006, 2006.

Morrison, H., Curry, J. A., and Khvorostyanov, V. I.: A new double-moment microphysics parameterization for application in cloud and climate models, Part I: Description, J. Atmos. Sci., 62, 1665–1677, https://doi.org/10.1175/JAS3446.1, 2005.

Morrison, H., hompson, G., and V. Tatarskii: Impact of cloud microphysics on the development of trailing stratiform precipitation in a simulated squall line: Comparison of one- and two-moment schemes, Mon. Weather Rev., 137, 991–1007, https://doi.org/10.1175/2008MWR2556.1, 2009.

Morrison, H., deBoer, G., Feingold, G., Harrington, J., Shupe, M., and Sulia, K.: Resilience of persistent Arctic mixed-phase clouds, Nat. Geosci., 5, 11–17, https://doi.org/10.1038/ngeo1332, 2012.

Murakami, M.: Numerical modeling of the dynamical and microphysical evolution of an isolated convective cloud–The July 19 1981 CCOPE cloud, J. Meteor. Soc. Jpn., 68, 107–128, https://doi.org/10.2151/jmsj1965.68.2_107, 1990.

Ovchinnikov, M., Korolev, A., and Fan, J.: Effects of ice number concentration on dynamics of a shallow mixed-phase stratiform cloud, J. Geophys. Res., 116, D00T06, https://doi.org/10.1029/2011JD015888, 2011.

Possner, A., Ekman, A. M. L., and Lohmann, U.: Cloud response and feedback processes in stratiform mixed-phase clouds perturbed by ship exhaust, Geophys. Res. Lett., 44, 1964–1972, https://doi.org/10.1002/2016GL071358, 2017.

Pruppacher, H. R. and Klett, J. D.: Microphysics of clouds and precipitation, 1st ed., D. Reidel Publishing Company, Dordrecht, Netherlands, 714 pp., ISBN 0-7923-4211-9, https://doi.org/10.1007/978-94-009-9905-3, 1978.

Ramaswamy, V., Boucher, O., Haigh, J., Hauglustaine, D., Haywood, J., Myhre, G., Nakajima, T., Shi, G. Y., and Solomon, S.: Radiative Forcing of Climate Change, in: Climate Change 2001: The Scientific basis, Contribution of working group I to the third assessment report of the intergovernmental panel on climate change, edited by: Houghton, J. T., Ding, Y., Griggs, D. J., Noguer, M., van der Linden, P. J., Dai, X., Maskell, K., and Johnson, C. A., Cambridge University Press, Cambridge, UK, and New York, NY, USA, 349–416, ISBN 0521807670, 2001.

Schima, J., McFarquhar, G., Romatschke, U., Vivekanandan, J., D'Alessandro, J., Haggerty, Wolff, C., Schaefer, E., Jarvinen, E., and Schnaiter, M.: Characterization of Southern Ocean boundary layer clouds using airborne radar, lidar, and in situ cloud data: Results from SOCRATES, J. Geophys. Res., 127, e2022JD037277, https://doi.org/10.1029/2022JD037277, 2022.

Seinfeld, J. H. and Pandis, S. N.: Atmospheric chemistry and physics: From air pollution to climate change, 1st ed., John Wiley & Sons, New York, NY, USA, 1326 pp., ISBN 9780471178163, 1998.

Solomon, A., de Boer, G., Creamean, J. M., McComiskey, A., Shupe, M. D., Maahn, M., and Cox, C.: The relative impact of cloud condensation nuclei and ice nucleating particle concentrations on phase partitioning in Arctic mixed-phase stratocumulus clouds, Atmos. Chem. Phys., 18, 17047–17059, https://doi.org/10.5194/acp-18-17047-2018, 2018.

Smagorinsky, J.: General circulation experiments with the primitive equations, Mon. Weather Rev., 91, 99–164, https://doi.org/10.1175/1520-0493(1963)091<0099:GCEWTP>2.3.CO;2, 1963.

Stevens, B. and Feingold, G.: Untangling aerosol effects on clouds and precipitation in a buffered system, Nature, 461, 607–613, https://doi.org/10.1038/nature08281, 2009.

Stevens, B., Lenschow, D. H., Faloona, I., Moeng, C.-H., Lilly, D. K., Blomquist, B., Vali, G., Bandy, A., Campos, T., Gerber, H., Haimov, S., Morley, B., and Thornton, D.: On entrainment rates in nocturnal marine stratocumulus, Q. J. Roy. Meteor. Soc., 129, 3469–3492, https://doi.org/10.1256/qj.02.202, 2003a.

Stevens, B., Lenschow, D. H., Vali, G., Gerber, H., Bandy, A., Blomquist, B., Brenguier, J.-L., Bretherton, C. S., Burnet, F., Campos, T., Chai, S., Faloona, I., Friesen, D., Haimov, S., Laursen, K., Lilly, D. K., Loehrer, S. M., Malinowski, S. P., Morley, B., Petters, M. D., Rogers, D. C., Russell, L., Savic-Jovcic, V., Snider, J. R., Straub, D., Szumowski, M. J., Takagi, H., Thornton, D. C., Tschudi, M., Twohy, C., Wetzel, M., and van Zanten, M. C.: Dynamics and chemistry of marine stratocumulus-DYCOMS-II, B. Am. Meteor. Soc., 84, 579–593, https://doi.org/10.1175/BAMS-84-5-579, 2003b.

Stephens, G. L. and Greenwald, T. J.: Observations of the Earth's radiation budget in relation to atmospheric hydrology. Part II: Cloud effects and cloud feedback, J. Geophys. Res., 96, 15325–15340, https://doi.org/10.1029/91JD00972,1991.

Tinel, C., Testud, J., Hogan, R. J., Protat, A., Delanoe, J., and Bouniol, D.: The retrieval of ice cloud properties from cloud radar and lidar synergy, J. Appl. Meteorol., 44, 860–875, https://doi.org/10.1175/JAM2240.1, 2005.

Tsushima, Y., Emori, S., Ogura, T., Kimoto, M., Webb, M. J., Williams, K. D., Ringer, M. A., Soden, B. J., Li, B., and Andronova, N.: Importance of the mixed-phase cloud distribution in the control climate for assessing the response of clouds to carbon dioxide increase: A multi-model study, Clim. Dynam., 27, 113–126, https://doi.org/10.1007/s00382-006-0127-7, 2006.

Tunved, P., Ström, J., and Krejci, R.: Arctic aerosol life cycle: linking aerosol size distributions observed between 2000 and 2010 with air mass transport and precipitation at Zeppelin station, Ny-Ålesund, Svalbard, Atmos. Chem. Phys., 13, 3643–3660, https://doi.org/10.5194/acp-13-3643-2013, 2013.

Twomey, S.: Pollution and the Planetary Albedo, Atmos. Environ., 8, 1251–1256, https://doi.org/10.1016/0004-6981(74)90004-3, 1974.

Warren, S. G., Hahn, C. J., London, J., Chervin, R. M., and Jenne, R. L.: Global distribution of total cloud cover and cloud types over land, NCAR Tech. Note NCAR/TN-273+STR, National Center for Atmospheric Research, Boulder, CO, 29 pp. + 200 maps, https://doi.org/10.2172/5415329 1986.

Wood, R.: Stratocumulus clouds, Mon. Weather Rev., 140, 2373–2423, https://doi.org/10.1175/MWR-D-11-00121.1, 2012.

Xue, L., Teller, A., Rasmussen, R. M., Geresdi, I., and Pan, Z.: Effects of aerosol solubility and regeneration on warm-phase orographic clouds and precipitation simulated by a detailed bin microphysical scheme, J. Atmos. Sci., 67, 3336–3354, https://doi.org/10.1175/2010JAS3511.1, 2010.

Zhang, D., Vogelmann, A., Kollias, P., Luke, E., Yang, F., Lubin, D., and Wang, Z.: Comparison of Antarctic and Arctic single-layer stratiform mixed-phase cloud properties using ground-based remote sensing measurements, J. Geophys. Res., 124, 10186–10204, https://doi.org/10.1029/2019JD030673, 2019.

Zheng, Y., Zhang, H., Rosenfeld, D., Lee, S. S., Su, T., and Li, Z.: Idealized Large-Eddy Simulations of Stratocumulus Advecting over Cold Water, Part I: Boundary Layer Decoupling, J. Atmos. Sci., 78, 4089–4102, https://doi.org/10.1175/JAS-D-21-0108.1, 2021.